European Journal of Taxonomy 1026: 30–64
https://doi.org/10.5852/ejt.2025.1026.3105
europeanjournaloftaxonomy.eu
ISSN 2118-9773
2025 · Neal L. *et al.*

Received: 8 August 2024 • *Accepted: 12 August 2025* • *Published: 11 November 2025*
Topic editor: Magalie Castelin • *Section editor: Nataliya Budaeva* • *Desk editor: Pepe Fernández*

Research article

urn:lsid:zoobank.org:pub:A9D6F837-22FC-4371-98CC-E1E6D6812BA8

New species of *Anguillosyllis* Day, 1963 (Annelida, Syllidae) from polymetallic nodule exploration areas, eastern Clarion-Clipperton Zone, central Pacific Ocean

Lenka NEAL[1,*], Regan DRENNAN[2], Helena WIKLUND[3], Eva C.D. STEWART[4], Muriel RABONE[5], Thomas G. DAHLGREN[6] & Adrian G. GLOVER[7]

[1,2,3,4,5,7] Life Sciences Department, Natural History Museum, London, SW7 5BD, UK.
[3,6] Department of Marine Sciences, University of Gothenburg, Box 463, 40530 Gothenburg, Sweden.
[3,6] Gothenburg Global Biodiversity Centre, Box 463, 40530 Gothenburg, Sweden.
[4] School of Ocean and Earth Sciences, University of Southampton, Southampton, SO14 3ZH, UK.
[6] NORCE Norwegian Research Centre, P.O.B. 22 Nygårdsgaten, NO-5838 Bergen, Norway.

[*]Corresponding author: l.nealova@nhm.ac.uk
[2] Email: r.drennan@nhm.ac.uk
[3] Email: helena.wiklund@marine.gu.se
[4] Email: e.stewart@nhm.ac.uk
[5] Email: m.rabone@nhm.ac.uk
[6] Email: thomas.dahlgren@marine.gu.se
[7] Email: a.glover@nhm.ac.uk

Abstract. The benthic annelid fauna of polymetallic nodule fields in the eastern Clarion-Clipperton Zone (CCZ), abyssal Central Pacific has recently been the subject of taxonomic investigations aiming to document the biodiversity of this region. While annelids are abundant and diverse within the CCZ, particularly high diversity was discovered within the syllid genus *Anguillosyllis* Day, 1963 from material collected during environmental surveys targeting exploration contract areas 'UK-1', 'OMS' and 'NORI-D', as well as Area of Particular Environmental Interest, 'APEI-6'. From the total *Anguillosyllis* material examined (134 specimens), 37 specimens were amenable to the formalization of three new species: *Anguillosyllis dalgleishae* sp. nov., *A. finnelli* sp. nov., and *A. villarae* sp. nov. Prior to this study, 20 species of *Anguillosyllis* were known worldwide and only two species were known from the CCZ – *A. truebloodi* Maciolek, 2020 and *A. hessleri* Maciolek, 2020.

Keywords. CCZ, deep-sea mining, taxonomic novelty, species distribution, molecular phylogeny, 18S, 16S, COI.

Neal L., Drennan R., Wiklund H., Stewart E.C.D., Rabone M., Dahlgren T.G. & Glover A.G. 2025. New species of *Anguillosyllis* Day, 1963 (Annelida, Syllidae) from polymetallic nodule exploration areas, eastern Clarion-Clipperton Zone, central Pacific Ocean. *European Journal of Taxonomy* 1026: 30–64.
https://doi.org/10.5852/ejt.2025.1026.3105

Introduction

The Clarion-Clipperton Zone (CCZ) polymetallic nodule area in the central abyssal Pacific Ocean has been explored in recent decades for its deep-sea mineral resources and their potential for commercial mining (e.g., Gollner *et al.* 2017; Glover *et al.* 2018; Jones *et al.* 2021; Smith *et al.* 2021). The exploration licenses are issued to Sponsoring States by the International Seabed Authority (ISA), which stipulates the need for environmental impact assessments and the establishment of preservation areas (Lodge *et al.* 2014; Jones *et al.* 2021; Washburn *et al.* 2021). Here, we concentrate on such studies within areas of the eastern CCZ prospected by 1) the UK Seabed Resources Ltd (UKSRL) exploration contract area 'UK-1', 2) the Ocean Mineral Singapore exploration contract area 'OMS', 3) Area of Particular Environmental Interest, 'APEI-6' and 4) Nauru Ocean Resources Inc (NORI) (a subsidiary of The Metals Company), which holds exploration rights to four areas (A, B, C and D) and is authorised to carry out its mineral exploration activities in the area of the Republic of Nauru.

Knowledge of the biodiversity and distribution of benthic taxa found within areas of potential mining operations is paramount to informed environmental impact assessments and conservation efforts (e.g., Smith *et al.* 2011, 2021; Jones *et al.* 2021; Rabone *et al.* 2023a, 2023b). Both biodiversity and species ranges remain poorly understood mainly due to under-sampling and the lack of comparable datasets produced by different research groups and contractors. The latter factor is compounded by the lack of formal taxonomic descriptions of the fauna, given that most represent species new to science. Sediment infauna, while comparatively better studied and to a higher resolution than other faunal categories such as nodule fauna or megafauna (Rabone *et al*. 2023a), cannot be captured by video or camera surveys limiting the size of the datasets. In general, annelid worms dominate the abyssal sediment macrofauna, constituting 50–75% of macrofaunal abundance and species richness, and are therefore considered a key component of benthic biodiversity (e.g., Glover *et al.* 2002; Smith *et al.* 2008; Stewart *et al*. 2023). Annelids also exhibit a broad range of feeding types and life-history strategies and are frequently used to evaluate anthropogenic disturbance in shallow-water habitats (Dean 2008). Thus, evaluation of the diversity and species ranges of annelid worms is critical to predicting and managing the impacts of nodule mining in the CCZ.

Our main objective has been to provide taxonomic and genetic data on macrofaunal annelids collected from the targeted areas within the CCZ. These data build on previous taxonomic works on annelid worms from the target areas (Wiklund *et al.* 2019, 2023; Drennan *et al.* 2021; Neal *et al.* 2022a, 2022b, 2023), as well as the wider CCZ area (e.g., Janssen *et al.* 2015; Bonifácio & Menot 2018; Blake 2019; Bonifácio *et al*. 2020, 2024; Maciolek 2020). Currently, 52 new annelid species have been formally described from the CCZ (Rabone *et al*. 2023b, 2024), with a focus on Spioniformia (Paterson *et al.* 2016; Guggolz *et al.* 2020; Neal *et al.* 2022a), Polynoidae Kinberg, 1856 (Bonifácio & Menot 2018), Cirratulidae Ryckholt, 1851 (Blake 2019), Opheliidae Malmgren, 1867, Scalibregmatidae Malmgren, 1867 and Travisiidae Hartmann-Schröder, 1971 (Wiklund *et al.* 2019), Nereididae Blainville, 1818 (Drennan *et al*. 2021), Amphinomida Lamarck, 1818 (Neal *et al*. 2022b) and Syllidae Grube, 1850 (Nilsson *et al.* 2024), including *Anguillosyllis* Day, 1963 (Maciolek 2020).

While targeting the annelid family Syllidae Grube, 1850, it has been noted that the majority of specimens found in the CCZ samples belong to the genus *Anguillosyllis*. *Anguillosyllis* is a rather enigmatic taxon within Syllidae, although its placement within this family based on morphology alone is ambiguous as it displays intermediate morphological characters between traditional Syllidae subfamilies (Aguado & San Martín 2008). The absence of pharyngeal armature has been observed in Anoplosyllinae Aguado & San Martín, 2009, while the smooth and long dorsal cirri are known in Eusyllinae Malaquin, 1893 and one pair of peristomial cirri, and ovate to papilliform antennae in Exogoninae Langerhans, 1879 (a subfamily in which *Anguillosyllis* was originally placed, based on *A*. *capensis* Day, 1963 having fused palps). Phylogenetic analyses, that incorporated both molecular and morphological data, recovered this genus as a basal sister taxon to all Syllidae (Aguado *et al.* 2012).

The genus was established for a single species, *Anguillosyllis capensis*, found in 183 m water depth off South Africa (Day 1963). The distinct appearance of this species due to characters such as short body and greatly elongated palps has made this species 'easy to recognize' and as a result it has been reported across a wide geographic and bathymetric range (Böggemann & Purschke 2005; Böggemann 2009). A further two species were assigned to *Anguillosyllis* by revisional work of Aguado & San Martín (2008). They examined specimens of *Braniella pupa* Hartman, 1965 from bathyal NW and SW Atlantic and *B. palpata* Hartman, 1967 from the Southern Ocean and noting the similarities between the two genera, declared *Braniella* Hartman, 1965 to be a junior synonym of *Anguillosyllis*. More recently, Barroso *et al.* (2017) described a new species, *A. lanai*, from 1035–2997 m on the continental slope off southeastern Brazil. Several undescribed species have also been reported in deep waters worldwide (e.g., Aguado *et al.* 2012; Langeneck *et al.* 2018; Neal *et al.* 2020; Gunton *et al.* 2021), suggesting that this enigmatic taxon may in fact be more common than previously thought.

An important contribution to the taxonomy of this genus was recently made by Maciolek (2020). Using collections from several deep-sea studies worldwide and examining ca 1400 specimens, Maciolek (2020) recognized and newly described 16 species, bringing the total number of species in the genus to 20. Her work provided further observations of morphological characters considered of taxonomic importance by previous workers (e.g., Aguado & San Martín 2008; Barroso *et al.* 2017) such as number of chaetigers in adults, degree of fusion of the palps, degree of development of parapodial lobes, structure and number of internal and external glands, number of chaetae in anterior chaetigers, shape and size of proventricle, annulation of the dorsum, and presence of four anal cirri.

Among the newly described species by Maciolek (2020), two were reported from the CCZ – *Anguillosyllis truebloodi* Maciolek, 2020 and *A. hessleri* Maciolek, 2020. However, up to four genetic lineages were recently found in specimens morphologically identified as *A. hessleri* (Drennan *et al*. 2025). Ongoing work suggests a much greater diversity of *Anguillosyllis* existing within the CCZ, with ~30 putative species recognized using a combination of morphological and/or molecular approaches (Neal pers. obs.). The majority of remaining putative species will be covered in a separate data publication (sensu Wiklund *et al*. 2023), as specimen damage and small numbers of individuals prevents full formal description of so many of these species. Here, we concentrate on the material amenable to taxonomic formalization, describing three new species: *Anguillosyllis dalgleishae* sp. nov., *A. finnelli* sp. nov., and *A. villarae* sp. nov., and providing a discussion of notable taxonomic characters in the genus.

Material and methods

Fieldwork

The first UKSR ABYSSLINE cruise (AB01) took place in October 2013 onboard the RV *Melville* and targeted the UK-1 exploration contract area (Fig. 1). The second cruise (AB02) took place in February-March 2015 onboard the RV *Thomas G. Thompson* and sampled a wider area (Fig. 1), including: UK-1 (depth ~4200 m) and OMS (depth ~4200 m) exploration contract areas, and APEI-6 (depth ~4050 m). The Resource Cruise 01 (RC01) took place aboard the MV *Pacific Constructor* between February and March 2020 and targeted exploration contract areas UK-1 and OMS (Fig. 1). Nauru Ocean Resources Inc. (NORI) Campaign 05a took place October to November 2020 and campaign 05d from April to June 2021, both onboard the *Maersk Launcher*, to the NORI-D exploration area (depth ~4300 m) (Fig. 1). Nauru Ocean Resources Inc. (NORI) Campaigns 07a and 07b took place onboard the Ocean Infinity vessel *Island Pride* in August 2022 and between November and December 2022, respectively (Fig. 1). The SMARTEX (Seabed Mining And Resilience To EXperimental impact) cruise JC241 took place between February and March 2023 onboard the RRS *James Cook* and sampled the Ocean Minerals Company (OMCO) 1979 mining collector test area (depth ~4700 m) (Fig. 1).

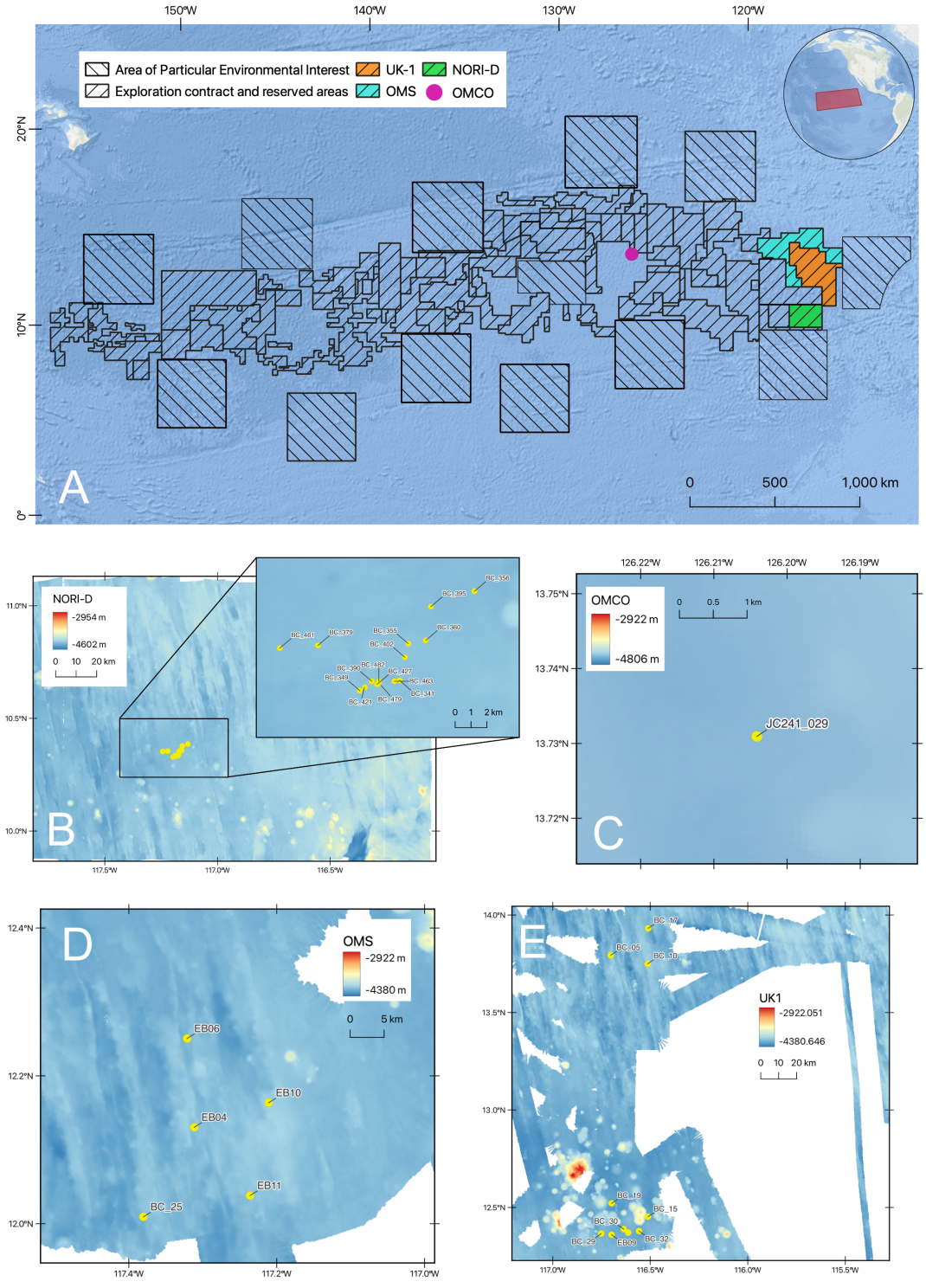

Fig. 1. Sampling sites showing occurrence of *Anguillosyllis* spp. **A**. Map of the nodule exploration contract areas, reserved areas, and Areas of Particular Environmental Interest (APEI) in the Clarion-Clipperton Zone (CCZ), central Pacific Ocean, showing the areas considered in this study (in colour), insert shows the position of CCZ to the continent. **B**. Nauru Ocean Resources Inc. license area D (NORI-D). **C**. Ocean Minerals Company (OMCO) 1979 mining collector test area. **D**. Ocean Minerals Singapore license area. **E**. UK seabed resources UK-1 license area.

For a comprehensive description of the methodological pipeline see Glover *et al.* (2016). Briefly, specimens were collected using box corers or a Brenke Epibenthic Sledge, with sediment sieved on 300 µm mesh size on board the vessels. Geographic data from sampling activities were recorded on a central GIS database (Fig. 1). Live-sorting of specimen samples was carried out onboard the vessels in a 'cold-chain' pipeline, with material maintained in chilled (2–4°C), filtered seawater. Specimens were assigned preliminarily identifications and imaged live using stereo microscopes with attached digital cameras (Glover *et al.* 2016). Specimens were then stored in individual microtube vials filled with aqueous solution of 80% non-denatured ethanol labelled appropriately and entered into a database. Samples were kept chilled throughout their transportation to the Natural History Museum, London, UK.

Morphological laboratory work

In the laboratory, preserved specimens were re-examined using stereo and compound microscopes with key morphological features photographed with digital camera. 'Shirlastain A' (SDL Atlas Textile Testing Solutions) was used during the morphological examination on some specimens, to ease observation of certain characters. Methyl Green stain was used to observe staining of internal glands. Scanning electron microscopy (SEM) using a SEM FEI Quanta 650 FEG was conducted on selected specimens (n = 3), following graded ethanol dehydration, critical point drying, and gold coating. Figures were assembled using Adobe Photoshop CS6 software.

Molecular laboratory work

Extraction of DNA was done with DNeasy Blood and Tissue Kit (Qiagen) using a Hamilton Microlab STAR Robotic Workstation, or with QuickExtract™ DNA extraction solution (Lucigen), following manufacturer guidelines, and adapted for a digestion time of 45 minutes. One nuclear gene (18S) and two mitochondrial genes (COI, 16S) were targeted for sequencing. Approximately 1800 bp of 18S were amplified using the primers 18SA 5′-AYCTGGTTGATCCTGCCAGT-3′ (Medlin *et al.* 1988) and 18SB 5′-ACCTTGTTACGACTTTTACTTCCTC-3′ (Nygren & Sundberg 2003). Around 450 bp of 16S were amplified with the primers ann16Sf 5′-GCGGTATCCTGACCGTRCWAAGGTA-3′ (Sjölin *et al.* 2005) and 16SbrH 5′-CCGGTCTGAACTCAGATCACGT-3′ (Palumbi 1996), and around 650 bp of COI (cytochrome *c* oxidase subunit 1) were amplified using LCO1490 5′-GGTCAACAAATCATAAAGATATTGG-3′ (Folmer *et al.* 1994) and COI-E 5′-TATACTTCTGGGTGTCCGAAGAATCA-3′ (Bely & Wray 2004) or polyLCO 5′-GAYTATWTTCAACAAATCATAAAGATATTGG-3′ and polyHCO 5′-TAMACTTCWGGGTGACCAAARAATCA-3′ (Carr *et al.* 2011).

The PCR mix for each reaction contained 10.5 µl of Red Taq DNA Polymerase 1.1X MasterMix (VWR), 0.5 µl of each primer (10 µm), and 1 µl of DNA template. PCR amplification profiles for each marker were as follows: 18S – initial denaturation of 5 mins at 95°C followed by 30 cycles of 30 s at 95°C, 1 min at 59°C, 2 min at 72°C, with a final extension of 2 min at 72°C; 16S – initial denaturation of 5 mins at 94°C followed by 35 cycles of 30s at 94°C, 30s at 57°C, 1 min at 68°C, with a final extension of 7 min at 68°C; COI – initial denaturation of 5 mins at 95°C followed by 35 cycles of 30 s at 95°C, 30 s at 49°C, 1 min at 74°C, with a final extension of 10 min at 74°C. PCR products were purified using a Millipore Multiscreen 96-well PCR Purification System, and sequencing was performed on an ABI 3730XL DNA Analyser (Applied Biosystems) at The Natural History Museum Sequencing Facility, using the same primers as in the PCR reactions plus two internal primers for 18S, 620F 5′-TAAAGYTGYTGCAGTTAAA-3′ (Nygren & Sundberg 2003) and 1324R 5′-CGGCCATGCACCACC-3′ (Cohen *et al.*1998). Overlapping sequence fragments were merged into consensus sequences using Geneious (Kearse *et al.* 2012) and aligned using MAFFT (Katoh 2002) for 18S and 16S, and MUSCLE (Edgar 2004) for COI, both programs used as plugins in Geneious, with default settings. COI alignments were translated into amino acids in order to check for stop codons and avoid the inclusion of pseudogenes. Sequences were compared against all COI, 16S, and 18S sequence data available on the public database GenBank (NCBI), using the blastn algorithm (Johnson *et al.* 2008) via the Geneious plugin with default settings.

Alignments were also created using all available CCZ *Anguillosyllis* sequences and all *Anguillosyllis* sequences available on GenBank. Distances within and between putative species of *Anguillosyllis* were calculated from these alignments using the p-distance and Kimura's two parameter (K2P) (Kimura 1980) models with default settings in MEGA ver. 11 (Tamura *et al.* 2021).

A combined Bayesian phylogenetic analysis of all three genes was conducted with MrBayes ver. 3.2.6 (Ronquist *et al.* 2012). This dataset included representatives of the three *Anguillosyllis* sp. nov. presented in this study, with representatives of the *Anguillosyllis* cf. *hessleri* complex (Drennan *et al.* 2025), and additional *Anguillosyllis* sequences and representative syllid outgroups from GenBank (Supp. file 1: Table S1). The most suitable substitution model for each gene was chosen using Modeltest-NG (Darriba *et al.* 2020) and the Bayesian information criterion (BIC) and adapted for MrBayes. The most suitable model for each gene position was GTR+I+G. Analyses were run for 10 million generations under default settings, with 2.5 million discarded as burnin. The IQ-TREE online web server tool (W-IQ-TREE, Trifinopoulos *et al*. 2016) was used to perform maximum likelihood (ML) phylogenetic analyses for the combined gene dataset and for separate 16S and COI alignments including all sequenced individuals of the three species of *Anguillosyllis* presented in this study. The best fitting models for these analyses were assessed and assigned automatically using the W-IQ-TREE ModelFinder function (Kalyaanamoorthy *et al*. 2017) using the Bayesian information criterion. Substitution models were as follows: combined 18S: TNe+G4, 16S: GTR+F+I+G4, COI: K3Pu+F+I+G4; separate 16S: GTR+F+I+G4; separate COI: TIM+F+I+G4. All ML analyses were conducted with 1000 bootstrap pseudoreplicates using the ultrafast bootstrap approximation algorithm (Minh *et al*. 2013; Hoang *et al*. 2018). All trees were visualized using FigTree ver. 1.4.4 (Rambaut 2018) and edited using Adobe Illustrator.

Nomenclatural assignments

Continuing the tradition of the NHM deep-sea research group, formalized species were named in honour of the scientists, technicians, and crew of the vessels used to collect them, with the names being randomly selected from a list of all on board. Type material, DNA specimen vouchers and DNA extractions are deposited at the Natural History Museum (NHM), London. A full list of all taxa including Natural History Museum Accession Numbers (NHMUK), NHM Molecular Collection Facility (NHM-MCF), and NCBI GenBank accession numbers is provided in Table 1.

Data handling

The field and laboratory work led to a series of databases and sample sets that were integrated into a 'data-management pipeline'. This included the transfer and management of data and samples between a central collections database, a molecular collections database and external repositories (GenBank, WoRMS, OBIS, GBIF, GGBN, ZooBank) through Darwin Core archives. This provides a robust data framework to support DNA taxonomy, in which openly available data and voucher material are key to quality data standards. A further elaboration of the data pipeline is published in Glover *et al.* (2016).

List of acronyms

ABYSSLINE	=	ABYSSal baseLINE
ANEA	=	Annelida
APEI	=	Area of Particular Environmental Interest
CCZ	=	Clarion-Clipperton Zone
ISA	=	International Seabed Authority
NHM	=	Natural History Museum London
NORI	=	Nauru Ocean Resources Inc.
OMCO	=	Ocean Minerals Company
OMS	=	Ocean Mineral Singapore

TMC	=	The Metals Company
UKSRL	=	UK Seabed Resources Ltd.
RC01	=	Resource cruise
SMARTEX	=	Seabed Mining And Resilience To EXperimental Impact

Results

Phylum Annelida Lamarck, 1802
Class Polychaeta Grube, 1850
Order Phyllodocida Dales, 1962
Family Syllidae Grube, 1850

Genus ***Anguillosyllis*** Day, 1963

Type species

Anguillosyllis capensis Day, 1963.

Diagnosis (amended from Maciolek 2020)

Body very small, adults with limited and fixed number of chaetigers (8–11). Palps elongated, free to the base or fused partly to completely. Prostomium with three antennae, without eyes. Peristomium with one pair of tentacular cirri similar to or smaller than prostomial antennae. Parapodia uniramous, with anterior and posterior lobes developed to varying degrees; with superior (dorsal) lobe that may be contractile. Dorsal cirri may be absent on a variable number of chaetigers, with true absence on chaetiger 2 or on all chaetigers except chaetiger 1. Compound chaetae heterogomph, with falcigers and spiniger-like blades. Falcigers uni- or bidentate. Pharynx straight, eversible, with two (or three) crowns or sections, external one formed by pharyngeal sheath, distal one surrounded by several (10–12) soft papillae, tooth absent. Proventricle cylindrical, usually tapered posteriorly, muscle rows obscure; with associated glandular structure wrapped around post-ventricle. Pygidium with four cirri, two lateral, two ventromedial.

Remarks

While the distinct look of *Anguillosyllis* (elongated palps, low number of chaetigers) might have contributed to the lumping of similar species in the past, the use of molecular techniques has revealed a far greater diversity within this genus than previously thought (Drennan *et al.* 2025). Recent taxonomic work reported on characters that could help differentiate between different species (Aguado & San Martín 2008; Barroso *et al.* 2017; Maciolek 2020). Most recently, Drennan *et al.* (2025**)** revealed novel and previously overlooked characters, best observed with the use of SEM, such as a complex form of prostomium, and absence of dorsal cirri on all but chaetiger 1. Here we rely predominantly on the characters used by Maciolek (2020), supplemented with SEM observations where possible. We caution against reliance on the characters such as size and shape of antennae or dorsal cirri, as these can differ even within a single specimen (Neal pers. obs.), likely due to preservation.

Update on previously reported characters

Palpal length can range from short (defined as similar in length to prostomium), to elongate (equaling multiple lengths of prostomium, usually no more than twice the length of prostomium), while **the shape of palps** can be pointed, conical or finger-like.

Prostomial antennae can vary in size (relative to prostomium and lateral antennae relative to median antenna) and in shape being papilliform, digitiform, club-shaped, cirriform or ovate, although caution is needed as stated above.

Table 1 (continued on next page). List of taxa presented in this paper with cruise record number, GUID (Global Unique Identifier link to data record at http://data.nhm.ac.uk), NHMUK accession number, NHMUK Molecular Collection Facility (MCf) sample ID number (NHMUK_MCF#) and NCBI GenBank accession number (Genbank#) for successfully sequenced genetic markers. GenBank numbers for phylogenetic analysis downloaded from GenBank are presented in Supp. file 2: Table S2.

Species	Specimen record no.	GUID	MCf no.	NHMUK reg. #	GenBank Acc. # COI/16S/18S
Anguillosyllis dalgleishae sp. nov.	NHM_837	42eab9a3-1d5c-43ec-86e2-4f5aa47bd5f1	0174126329	ANEA 2024.2686 (paratype)	…./PV579009/…
Anguillosyllis dalgleishae sp. nov.	NHM_1021	d5d9b8f4-8717-43e7-9e6f-422ce4acfdb6	0174126318	ANEA 2024.2687	…/PV579010/…
Anguillosyllis dalgleishae sp. nov.	NHM_1201	889e12a1-6e88-4987-9e8a-1d758fd43ea3	0174126305	ANEA 2024.2688	…/PV579011/…
Anguillosyllis dalgleishae sp. nov.	NHM_1347A	4be32c49-79e4-4cb1-a7b2-12b6265ff348	0174126294	ANEA 2024.2689 (paratype)	PV577541/PV579012/…
Anguillosyllis dalgleishae sp. nov.	NHM_1508C	502bcd95-9ec8-4ed2-acea-e630ede84474	0174126281	ANEA 2024.2690	PV577525/PV579013/…
Anguillosyllis dalgleishae sp. nov.	NHM_1597	f4490e8c-6091-4f27-85df-982e78912412	0174126245	ANEA 2024.2691	…/PV579014/…
Anguillosyllis dalgleishae sp. nov.	NHM_1657	e40b2e1f-f476-4085-9993-6dcf1221d8ad	0174126270	ANEA 2024.2692	…/PV579015/…
Anguillosyllis dalgleishae sp. nov.	NHM_1773	589cb9f8-292c-4668-940d-b2891384e4c0	0174126328	ANEA 2024.2693	…/PV579016/…
Anguillosyllis dalgleishae sp. nov.	NHM_1773A	fb1eb56d-569c-4f11-83d0-8c60ced37856	0174126246	ANEA 2024.2694	…/PV579017…
Anguillosyllis dalgleishae sp. nov.	NHM_1867	7195bc27-fb46-4f87-8c76-48266394b848	0174126319	ANEA 2024.2695 (holotype)	…/PV579018/…
Anguillosyllis dalgleishae sp. nov.	NHM_1990	d6d4cdd0-e6ab-4e61-b9b0-e2eb3881e64a	0174126304	ANEA 2024.2696	…/PV664892/…
Anguillosyllis dalgleishae sp. nov.	NHM_1669A	b6584f26-950c-4506-b7e0-aec9cd37c46e	0174126257	ANEA 2024.2697 (paratype)	…/PV579019/…
Anguillosyllis dalgleishae sp. nov.	NHM_4729_ ECDS5	9f76d801-e1bb-42d2-830d-0caec6103f72	0174126254	ANEA 2024.2698	…/…/PV579029
Anguillosyllis dalgleishae sp. nov.	NHM_4731_ ECDS2	2cb21b0d-bbf1-4c9e-a04e-728c72a9041d	0174126273	ANEA 2024.2699	…/PV579020/…
Anguillosyllis villarae sp. nov.	NHM_5657	c382ab84-7641-40bb-91db-107aa41c8eee	0174126296	ANEA 2024.2701 (paratype)	PV577533/…/…
Anguillosyllis villarae sp. nov.	NHM_8730	71da1d0f-f4b9-4390-a8de-4c55e8351ad0	0174126248	ANEA 2024.2702	PV577534/…/…
Anguillosyllis villarae sp. nov.	NHM_8730B	290627ed-657b-4965-a9bd-920e8ca878ce	0174126303	ANEA 2024.2703	PV577535/…/PV579031
Anguillosyllis villarae sp. nov.	NHM_8811	aa8735af-ee3a-456f-bc57-888dd874e7fc	0174126322	ANEA 2024.2704 (holotype)	PV577536/PV579024/ PV579032
Anguillosyllis villarae sp. nov.	NHM_5908	bc633595-9ba5-4320-a0c8-e0022060eac7	0174126247	ANEA 2024.2705	…/PV579025/…

Table 1 (continued).

Species	Specimen record no.	GUID	MCf no.	NHMUK reg. #	GenBank Acc. # COI/16S/18S
Anguillosyllis villarae sp. nov.	NHM_7689B	2280eace-04fb-430a-aa3f-d2163f629c86	0174126320	ANEA 2024.2706 (paratype)	PV577537/…/…
Anguillosyllis villarae sp. nov.	NHM_9396_ HW18	d38da487-db2d-4274-bc96-ba7af0112e02	0174126278	ANEA 2024.2707	PV577538/…/…
Anguillosyllis villarae sp. nov.	NHM_10276	82b4921b-0ff9-4337-9bc4-034367e808c5	0174123627	ANEA 2024.2708	PV577539/…/…
Anguillosyllis villarae sp. nov.	NHM_10374_ CB12	fe6b7444-31bf-400f-9ed1-66530bb53a8c	0174126302	ANEA 2024.2709	PV577540/…/…
Anguillosyllis villarae sp. nov.	NHM_7227A	45112357-3af9-4c7f-8c93-d014c68f64ca	0174126280	ANEA 2024.2710	…/PV579026/…
Anguillosyllis villarae sp. nov.	NHM_6940	50527b56-3f4d-430f-929b-fa4d91b1d858	0174126295	ANEA 2024.2711	…/PV579027/…
Anguillosyllis villarae sp. nov.	NHM_5399	8a50f3cb-93de-4aa6-8792-cac45d2b2137	0174126271	ANEA 2024.2712	…/PV579028/…
Anguillosyllis finnelli sp. nov.	NHM_5880	654e0cbb-ac72-4aec-93b0-a24302d3e16c	0174126256	ANEA 2024.2713 (paratype)	PV664495/…/…
Anguillosyllis finnelli sp. nov.	NHM_4733_ ECDS4	89b42808-8b28-431e-b4d1-7c7b486289b7	0174126249	ANEA 2024.2714	PV577526/PV579021/…
Anguillosyllis finnelli sp. nov.	NHM_4741_ ECDS4	c2db9a70-9ccb-4d7e-abbf-4bef0404844c	0174126325	ANEA 2024.2715	…/PV579022/…
Anguillosyllis finnelli sp. nov.	NHM_8801_ HW03	04898df3-ab82-4b5d-8c82-7f0a5a396eac	0174126279	ANEA 2024.2716	PV577527/…/…
Anguillosyllis finnelli sp. nov.	NHM_8730A	c3b77851-d8d0-4a33-9f2b-2a993391f41d	0174126320	ANEA 2024.2717 (paratype)	PV577528/…/…
Anguillosyllis finnelli sp. nov.	NHM_8783_ HW01	68b5e2d7-8061-4f19-adad-b577c49fb335	0174126255	ANEA 2024.2718	PV577529/…/…
Anguillosyllis finnelli sp. nov.	NHM_8789_ HW05	8a93a352-604b-420f-b328-930c84d540cf	0174126272	ANEA 2024.2719	PV664496/…/…
Anguillosyllis finnelli sp. nov.	NHM_093	6d7ef8a1-9fa4-4eec-aca2-f68b1ace677b	0174126258	ANEA 2024.2720 (holotype)	PV577530/PV579023/ PV579030
Anguillosyllis finnelli sp. nov.	NHM_10602_ GB01	f7d6faae-4c53-4fcd-a168-e55f53d3201c	0174126301	ANEA 2024.2721	PV577531/…/…
Anguillosyllis finnelli sp. nov.	NHM_10334_ CB3	15c30fcb-cfdb-46c1-9066-f6eb52c4eb09	0174126326	ANEA 2024.2722	PV577532/…/…
Anguillosyllis finnelli sp. nov.	NHM_10372_ CB06	1cd18a15-4081-482f-b380-418cbe9a20e9	0174126321	ANEA 2024.2723	PV664497/…/…

Tentacular cirri can range in size and shape similar to diversity of shape displayed by the antennae. **Parapodia** themselves can differ in length, and in shape, size and development of the associated parapodial lobes/projections. **Ventral cirri** showed some variation in length, thickness and the point of insertion on parapodium (median or subdistal).

Presence/absence of dorsal cirri on chaetiger 2 was discussed by Barroso *et al.* (2017) and Maciolek (2020) as an important character. Although dorsal cirri on chaetiger 2 are only rarely confirmed (they may be either absent or lost), the type species of the genus, *A. capensis* was originally described as bearing dorsal cirri on all chaetigers (Day 1963). However, the presence of the dorsal cirri on chaetiger 2 was not confirmed by examination of the holotype NHMUK.1963.1.29, which is in extremely poor shape (Fig. 2). Maciolek (2020) reported the presence of dorsal cirri on chaetiger 2 on two specimens of *A. palpata* (Hartman, 1967) and one specimen of *A. hampsoni* Maciolek, 2020, with basal cirrophores also observed on chaetiger 2 in *A. truebloodi*. No specimens examined from UKSR material in the present study or previous study (Drennan *et al.* 2025) bore dorsal cirri on the second chaetiger.

True absence of dorsal cirri in other chaetigers. The true absence of dorsal cirri on chaetiger 2 has already been discussed above. Interestingly, SEM revealed true absence in all chaetigers but chaetiger 1 in *Anguillosyllis dalgleishae* sp. nov. This character state was already reported by Drennan *et al.* (2025) in *Anguillosyllis* cf. *hessleri* from the CCZ. Previously, based solely on examination using light microscopy, Maciolek (2020) suggested that in the following species the dorsal cirri are "missing" in all but chaetiger 1: *Anguillosyllis acsara* Maciolek, 2020, *A. hadra* Maciolek, 2020, *A. taleola* Maciolek, 2020, *A. elegantissima* Maciolek, 2020, *A. enneapoda* Maciolek, 2020, *A. hessleri*, *A. inornata* Maciolek, 2020 and *A. sepula* Maciolek, 2020.

Prostomium has been given little attention in previous descriptions, usually described in simple terms such as dome-shaped, rounded, pentagonal, longer than wide, as long as wide etc. Based on observations from light microscopy, Maciolek (2020) reported that three species *A. carolina* Maciolek,

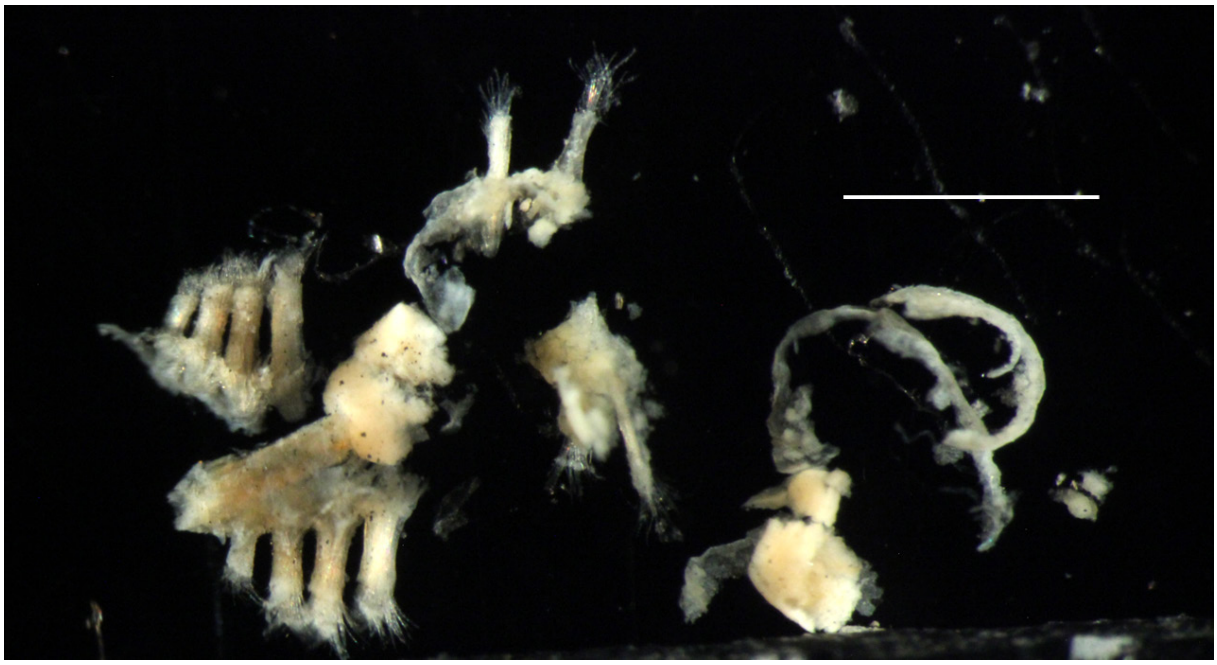

Fig. 2. *Anguillosyllis capensis* Day, 1963, holotype (NHMUK.1963.1.29) in its current state. Scale bar = 1 mm.

2020, *A. denaria* Maciolek, 2020 and *A. taleola* appear to have the prostomium in two parts. Our SEM observations showed that the prostomium is a complex structure composed of superimposed lobes of variable shapes, which may potentially differentiate species (see also Drennan *et al.* 2025).

Chaetae. Chaetae were previously considered falcigerous or spiniger-like, with variable length of blades, development of serration and number per chaetiger. Previously, only *A. palpata* was considered to have unique distinctly hooked chaetae (Maciolek 2020), with slightly hooked tips reported in *A. truebloodi* and *A. hampsoni* by Maciolek (2020). Our observations confirmed the presence of bidentate chaetae in *Anguillosyllis villarae* sp. nov. for the first time in this genus. Additionally, chaetal blades in *Anguillosyllis* can vary in thickness from narrow to flat and wide. The shafts of falcigerous chaetae in several anterior chaetigers in some species have been found to be denticulated, with denticles arranged in horizontal rows.

Internal glands. Maciolek (2020) reported on the shape and size of internal glands within parapodia, but we have found these difficult to observe and quantify. A stained circle of cells post-ventricle was observed when specimens were stained with Methyl Green (Neal pers. obs.).

Anguillosyllis dalgleishae sp. nov.
urn:lsid:zoobank.org:act:9A52883F-A914-4190-8B89-10E9834ACA9E
Figs 3–5, 6A

Diagnosis

Body with 10 chaetigers. Prostomium in two parts, with three short antennae. Palps elongated, fused for at most ⅓–⅔ of their length. Parapodia with large conical dorsal lobes (flaps). Dorsal cirri on chaetiger 1 only. Heterogomph chaetae unidentate.

Etymology

The species name is dedicated to Claire Dalgleish, benthic operations lead on all cruises to the NORI-D area (C5a, C5d, C7a, C7b).

Material examined

Holotype

PACIFIC OCEAN – **Eastern Central Pacific, Clarion Clipperton Fracture Zone** • 12.0415° N, 117.2171667° W; 4094 m depth; 13 Mar. 2015; A.G. Glover, H. Wiklund, T. Dahlgren and M. Brasier leg.; Brenke Epibenthic Sledge; specimen GUID: 7195bc27-fb46-4f87-8c76-48266394b848; field ID; NHM_01867; GenBank 16S gene: PV579018; NHMUK ANEA 2024.2695.

Paratypes

PACIFIC OCEAN – **Eastern Central Pacific, Clarion Clipperton Fracture Zone** • 1 spec.; 12.37098333° N, 116.61365° W; 4160 m depth; 21 Feb. 2015; A.G. Glover, H. Wiklund, T. Dahlgren and M. Brasier leg.; USNEL Box Core; specimen GUID: 42eab9a3-1d5c-43ec-86e2-4f5aa47bd5f1; field ID NHM_00837; GenBank 16S gene: PV579009; NHMUK ANEA 2024.2686 • 1 spec.; 12.25733333° N, 117.3021667° W; 4302 m depth; 1 Mar. 2015; A.G. Glover, H. Wiklund, T. Dahlgren and M. Brasier leg.; Brenke Epibenthic Sledge; specimen GUID: 4be32c49-79e4-4cb1-a7b2-12b6265ff348; field ID NHM_01347A; GenBank COI gene: PV577541; 16S gene: PV579012; NHMUK ANEA 2024.2689 • 1 spec.; 12.3635° N, 116.681° W; 4233 m depth; 10 Mar. 2015; A.G. Glover, H. Wiklund, T. Dahlgren and M. Brasier leg.; Brenke Epibenthic Sledge; specimen GUID: b6584f26-950c-4506-b7e0-aec9cd37c46e; field ID NHM_01669A; GenBank 16S gene: PV579019; NHMUK ANEA 2024.2697.

Other material

PACIFIC OCEAN – **Eastern Central Pacific, Clarion Clipperton Fracture Zone** • 1 spec.; 12.13366667° N, 117.292° W; 4122 m depth; 24 Feb. 2015; A.G. Glover, H. Wiklund, T. Dahlgren and M. Brasier leg.; Brenke Epibenthic Sledge; specimen GUID: d5d9b8f4-8717-43e7-9e6f-422ce4acfdb6; field ID NHM_01021; GenBank 16S gene: PV579010; NHMUK ANEA 2024.2687 • 1 spec.; 12.00945° N, 117.1781167° W; 4144 m depth; 27 Feb. 2015; A.G. Glover, H. Wiklund, T. Dahlgren and M. Brasier leg.; USNEL Box Core; specimen GUID: 889e12a1-6e88-4987-9e8a-1d758fd43ea3; field ID NHM_01201; GenBank 16S gene: PV579011; NHMUK ANEA 2024.2688 • 1 spec.; 12.45178333° N, 116.5122667° W; 4196 m depth; 4 Mar. 2015; A.G. Glover, H. Wiklund, T. Dahlgren and M. Brasier leg.; USNEL Box Core; specimen GUID: 502bcd95-9ec8-4ed2-acea-e630ede84474; field ID NHM_01508C; GenBank COI gene: PV577525; 16S gene: PV579013; NHMUK ANEA 2024.2690 • 1 spec.; 12.52121667° N, 116.69815° W; 4237 m depth; 8 Mar. 2015; A.G. Glover, H. Wiklund, T. Dahlgren and M. Brasier leg.; USNEL Box Core; specimen GUID: f4490e8c-6091-4f27-85df-982e78912412; field ID NHM_01597; GenBank 16S gene: PV579014; NHMUK ANEA 2024.2691 • 1 spec.; 12.3635° N, 116.681° W; 4233 m depth; 10 Mar. 2015; A.G. Glover, H. Wiklund, T. Dahlgren and M. Brasier leg.; Brenke Epibenthic Sledge; specimen GUID: e40b2e1f-f476-4085-9993-6dcf1221d8ad; field ID NHM_01657; GenBank 16S gene: PV579015; NHMUK ANEA 2024.2692 • 1 spec.; 12.17383333° N, 117.1928333° W; 4045 m depth; 11 Mar. 2015; A.G. Glover, H. Wiklund, T.vDahlgren and M. Brasier leg.; Brenke Epibenthic Sledge; specimen GUID: 589cb9f8-292c-4668-940d-b2891384e4c0; field ID NHM_01773; GenBank 16S gene: PV579016; NHMUK ANEA 2024.2693 • 1 spec.; 12.17383333° N, 117.1928333° W; 4045 m depth; 11 Mar. 2015; A.G. Glover, H. Wiklund, T. Dahlgren and M. Brasier leg.; Brenke Epibenthic Sledge; specimen GUID: fb1eb56d-569c-4f11-83d0-8c60ced37856; field ID NHM_01773A; GenBank 16S gene: PV579017; NHMUK ANEA 2024.2694 • 1 spec.; 12.00931667°vN, 117.3803° W; 4141 m depth; 15 Mar. 2015; A.G. Glover, H. Wiklund, T. Dahlgren and M. Brasier leg.; USNEL Box Core; specimen GUID: d6d4cdd0-e6ab-4e61-b9b0-e2eb3881e64a; field ID NHM_01990; GenBank 16S gene: PV664892; NHMUK ANEA 2024.2696 • 1 spec.; 13.93242102° N, 116.5110797° W; 4143.62 m depth; 5 Mar. 2020; A.G. Glover, H. Wiklund, G. Bribiesca Contreras and E. Simon Lledó leg.; USNEL Box Core; specimen GUID: 9f76d801-e1bb-42d2-830d-0caec6103f72; field ID NHM_04729_ESDS5; GenBank 18S gene: PV579029; NHMUK ANEA 2024.2698 • 1 spec.; 12.37908954° N, 116.5576715° W; 4196.02 m depth; 11 Mar. 2020; A.G. Glover, H. Wiklund, G. Bribiesca Contreras and E. Simon Lledó leg.; USNEL Box Core; specimen GUID: 2cb21b0d-bbf1-4c9e-a04e-728c72a9041d; field ID NHM_04731_ECDS2; GenBank 16S gene: PV579020; NHMUK ANEA 2024.2699.

Description

Measurements and appearance. Relatively large sized species, up to 3.25 mm in length for 10 chaetigers (Fig. 3B–C). Holotype NHMUK ANEA 2024.2695, posteriorly complete, 3.25 mm long and 0.45 mm wide at widest point for 10 chaetigers; right parapodia 9–10 removed for tissue sampling for DNA analysis. Paratype NHMUK ANEA 2024.2689, posteriorly complete, 2 mm long and 0.3 mm wide for 10 chaetigers, pygidial cirri missing, two left parapodia removed for tissue sampling for DNA analysis. Paratype NHMUK ANEA 2024.2697, posteriorly complete, 3 mm long and 0.4 mm wide for 10 chaetigers, pygidial cirri missing, three left parapodia removed for tissue sampling for DNA analysis. Paratype NHMUK ANEA 2024.2686, SEM specimen on stub (Fig. 4A–G), posteriorly incomplete and damaged, ~2 mm long and 0.3 mm wide for about 8 chaetigers. Other specimens in variable condition due to preservation or tissue sampling for DNA analysis; five specimens posteriorly complete with 10 chaetigers, ranging in length from 2 mm to 3 mm and up to 0.4 mm at widest point. Body relatively straight, tapering only at the first segment anteriorly, and from the pygidium posteriorly. Live specimen semi-translucent, without pigmentation (Fig. 3A); fixed specimen opaque, creamy white in ethanol (Fig. 3B–C).

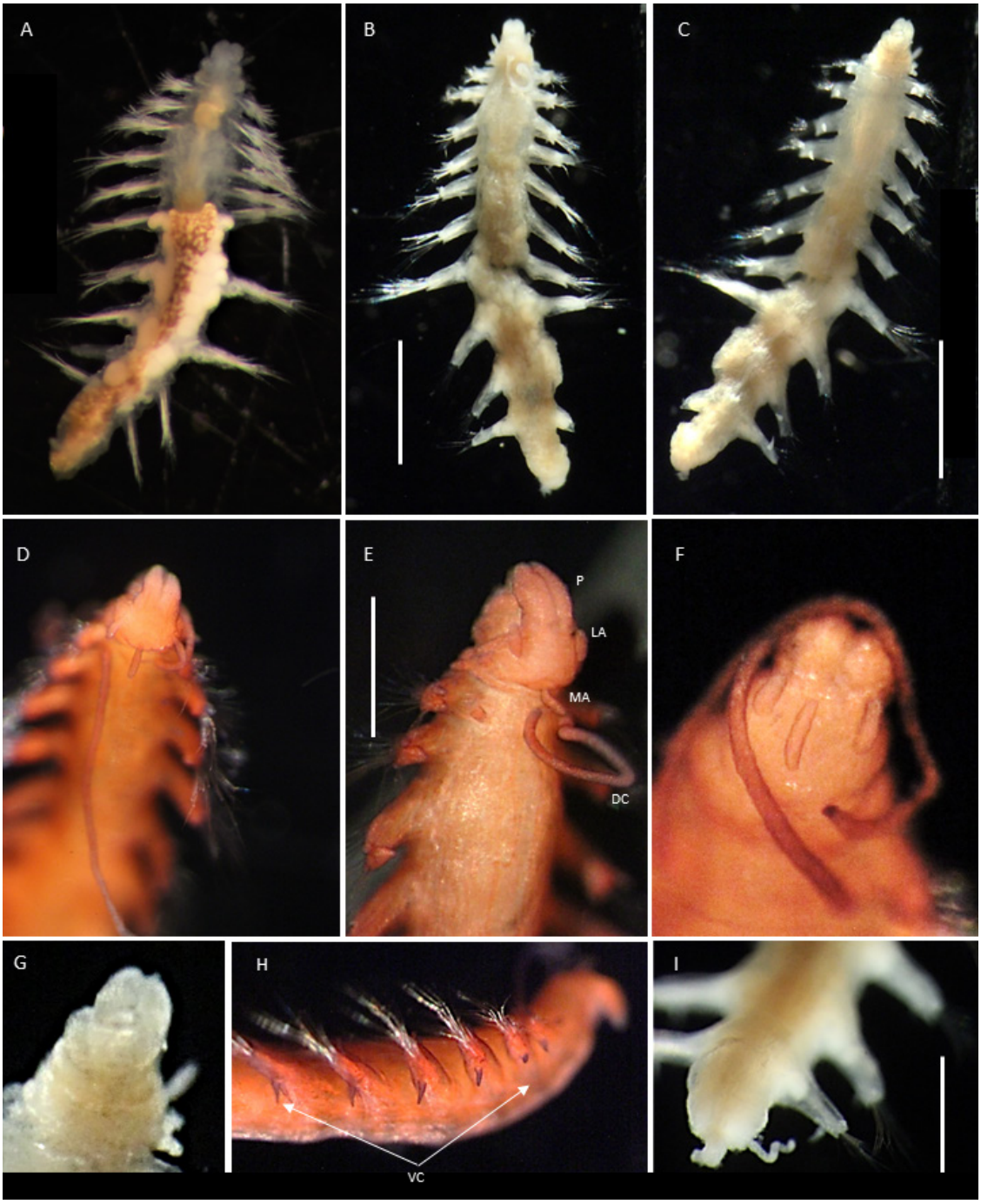

Fig. 3. *Anguillosyllis dalgleishae* sp. nov. **A**. Complete live specimen (NHMUK ANEA 2024.2692) in dorsal view, with eggs visible in the posterior part of the body. **B–C, E, G**. Holotype (NHMUK ANEA 2024.2695). **B**. Preserved specimen in dorsal view. **C**. Preserved specimen in ventral view. **D**. Paratype (NHMUK ANEA 2024.2689), anterior end in dorsal view with palps, antennae, dorsal cirri; specimen stained with Shirlastain A. **E**. Anterior end in dorsolateral view; specimen stained with Shirlastain A. **F, H–I**. Paratype (NHMUK ANEA 2024.2697), detail of antennae; specimen stained with Shirlastain A. **G**. Ventral view of partially extended proboscis. **H**. Ventrolateral view of anterior part of the body with ventral cirri (arrows); specimen stained with Shirlastain A. **I**. Terminal anal cirri. Abbreviations: DC = dorsal cirri; LA = lateral antennae; MA = median antenna; P = palps; VC = ventral cirri. Scale bars: B–C = 1 mm; E, I = 500 µm.

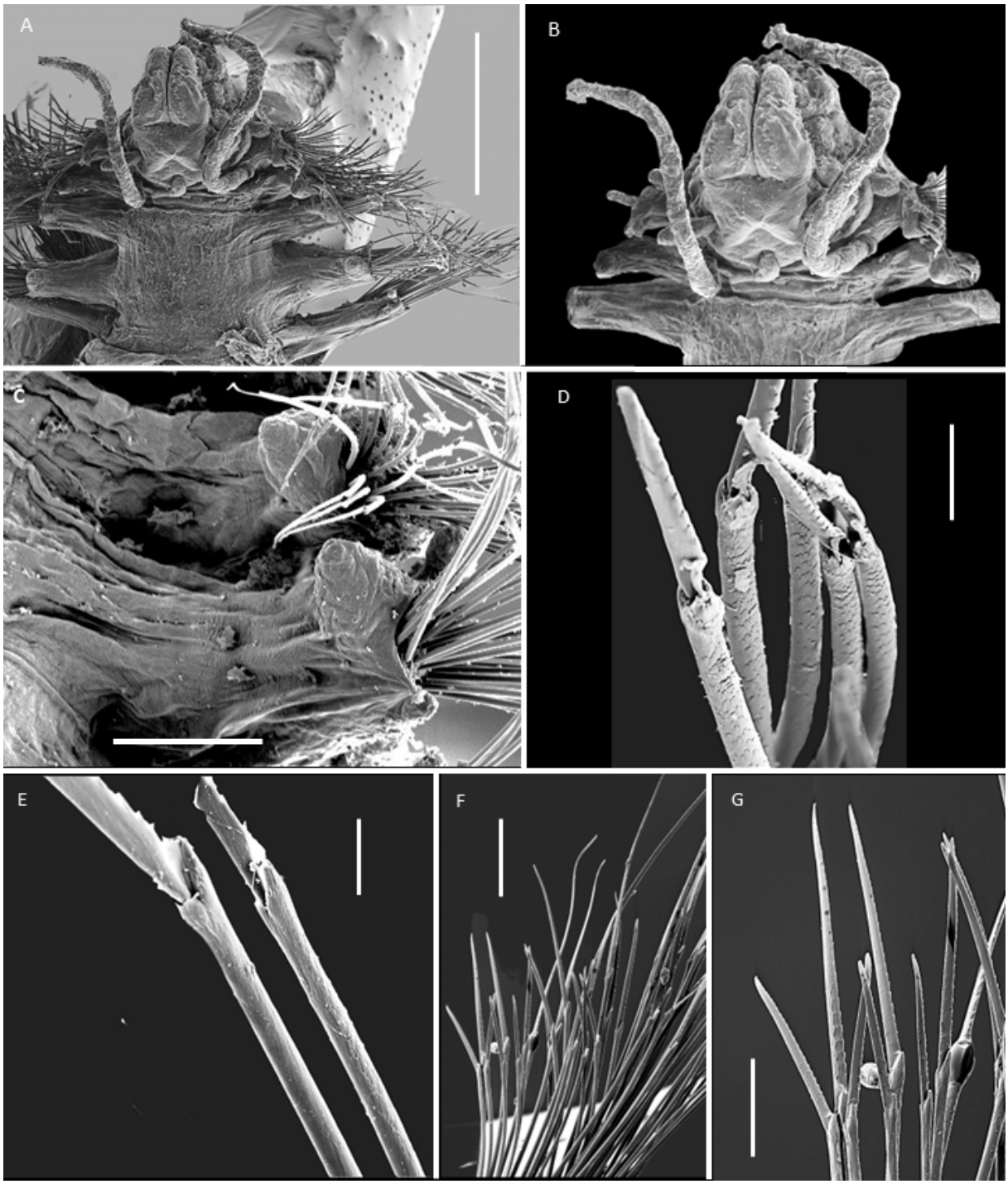

Fig. 4. *Anguillosyllis dalgleishae* sp. nov., paratype (NHMUK ANEA 2024.2686), SEM micrographs. **A**. Detail of the anterior end in dorsal view. **B**. Detail of prostomium and palps in dorsal view. **C**. Large dorsal lobes, parapodia 3 and 4. **D**. Falcigerous chaetae of chaetiger 1 with denticulated shafts. **E**. Falcigerous chaetae of chaetiger 5 with smooth or indistinctly denticulated shafts. **F**. Bundle of chaetae from 7th parapodium. **G**. Blades of compound chaetae from the 7th parapodium. Scale bars: A = 300 µm; C = 50 µm; D = 5 µm; E = 10 µm; F = 50 µm; G = 30 µm.

Prostomium. Rounded, slightly wider than long under light microscope (Figs 3D, 5A-inset); SEM shows differentiation into median quadrate lobe with deep notch on the posterior margin superimposed onto inferior rounded lobe (Figs 4A–B, 6A). Eyes absent. Prostomium bearing three short, digitiform antennae and two palps (Figs 3D–F, 4A–B, 5A-inset). Antennae just under the length of the prostomium, with the median antenna slightly longer than lateral antennae and inserted posterio-dorsally on the prostomium; lateral antennae inserted more anteriorly. Palps smooth, somewhat elongate, approximately 1½ the length of the prostomium, and conical to somewhat finger-like in shape; palps sharply arcing ventrally from the base in almost all specimens and fused for at most ½–⅔ their length (degree of fusion not particularly clear) with distinct midline furrow and acute distal notch.

Tentacular segment. Achaetous, bearing two short ovate tentacular cirri, approximately ½ the length of the antennae and inserted laterally (Fig. 5A). Pharyngeal tube extending to chaetigers 2–3; proventricle spanning from chaetigers 2–4, barrel to lightbulb-shaped, tapered posteriorly, with possibly ~15–20 muscle cell rows, though this is difficult to discern through body wall of preserved specimens (Fig. 3B–C) and best observed in live specimen (Fig. 3A). Partially everted pharynx observed in only one specimen (Fig. 3G).

Parapodia. Somewhat short, rounded rectangular, and uniramous, with posterior-most two chaetigers somewhat thinner than on previous segments. Parapodia with large conical dorsal lobe (Figs 4C, 5C) and two short, papilliform lobes (Fig. 5A–C); posterior lobes smaller than anterior lobes on anterior-most

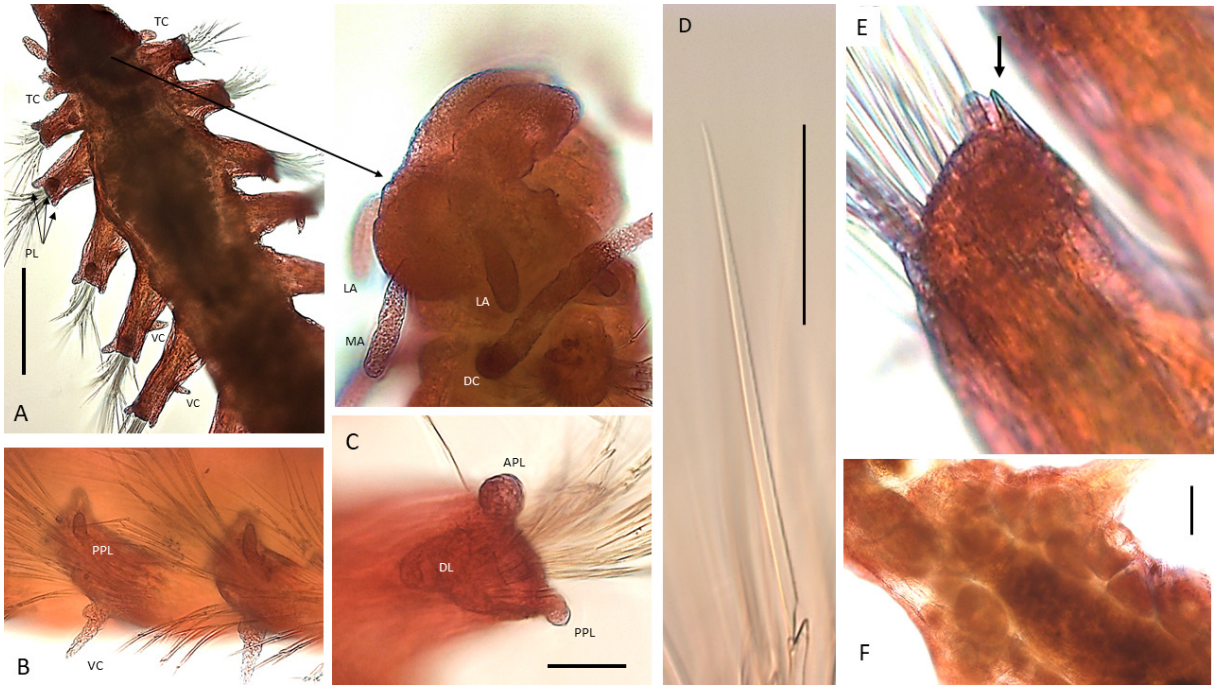

Fig. 5. *Anguillosyllis dalgleishae* sp. nov., specimens stained with Shirlastain A. **A, C–D, F**. Holotype (NHMUK ANEA 2024.2695). **A**. Anterior end in dorsal view, inset marked by arrow with detail of prostomium and palps in dorsolateral view. **B**. Paratype (NHMUK ANEA 2024.2689), parapodia with parapodial lobes and ventral cirri. **C**. Detail of parapodial lobes. **D**. Spiniger-like chaeta from chaetiger 1. **E**. Specimen NHMUK ANEA 2024.2692, aciculum (marked by arrow). **F**. Eggs seen through body wall. Abbreviations: APL = anterior parapodial lobe; DC = dorsal cirri; DL = dorsal lobe; LA = lateral antenna; MA = median antenna; PL = parapodial lobes; PPL = posterior parapodial lobe; TC = tentacular cirri; VC = ventral cirri. Scale bars: A, D, F = 50 µm; C = 25 µm.

chaetigers (Fig. 5C), but developed moving posteriorly, becoming subequal in length to the anterior lobe around chaetiger 6, and slightly exceeding the anterior lobe in size on subsequent chaetigers. Dorsal cirri present only on chaetiger 1, where long, filiform (Figs 3D–F, 4A–B, 5A-insert); absent in other chaetigers. Ventral cirri short and conical with an expanded base, inserted midway along the parapodia (Figs 3H, 5A–B). Several pointed acicula per parapodium visible, with tips non emergent (Fig. 5E, marked by arrow). Each parapodium bearing dense bundles of numerous compound heterogomph chaetae, bundles becoming slightly sparser moving posteriorly, chaetae falcigerous to spiniger-like (Fig. 4F–G). Falcigerous chaetae of chaetigers 1–4 with denticulated shafts, with denticles arranged in irregular horizontal rows (Fig. 4D), from chaetiger 5 with shafts indistinctly denticulated or smooth (Fig. 4E). Blades finely serrated, unidentate decreasing in length dorso-ventrally, ranging from elongate, slender spiniger-like to shorter falcigers (Figs 4F–G, 5D), with blades of the longest spiniger-like chaetae 230–250 µm, and shortest falcigers 25–30 µm; chaetae emerge from semicircular flap that extends from posterior lobe ventrally towards the base of the parapodium.

Pygidium. Conical to rounded; with four appendages; lateral cirri missing, ventromedial often missing, when present long, curled and filiform (Fig. 3I).

Reproductive information

Three specimens ovigerous; eggs visible through body cavity wall in all specimens between chaetigers 6–10, eggs irregularly shaped, ~50 µm in diameter (Figs 3A, 5F).

Genetic data

Specimens (n = 14) assigned to *A. dalgleishae* sp. nov. form a clade (Supp. file 3: Fig. S1, Supp. file 4: Fig. S2), with low intraspecific divergence across all sequences (maximum intraspecific p-distance/K2P 0.5/0.5% for 16S and 1.3/1.3% for COI). Sequences matched with high % identity (99.7–100%) in blastn search and 0–0.3% in both p-distance and K2P to a 16S sequence of an unidentified *Anguillosyllis* specimen (accession number: MK971075; ID: *Anguillosyllis* sp. 43 PB voucher 021-BGR-0045) (see Fig. 7) collected from the BGR contract area of the Eastern CCZ, published in Bonifácio *et al.* (2020). In terms of the nuclear 18S gene, *A. dalgleishae* was also well defined, differing from other *Anguillosyllis* sequences by a minimum of five (*A.* cf. *hessleri* sp. NHM_552 NHMUK2024.1002, *A. capensis* ZMH_

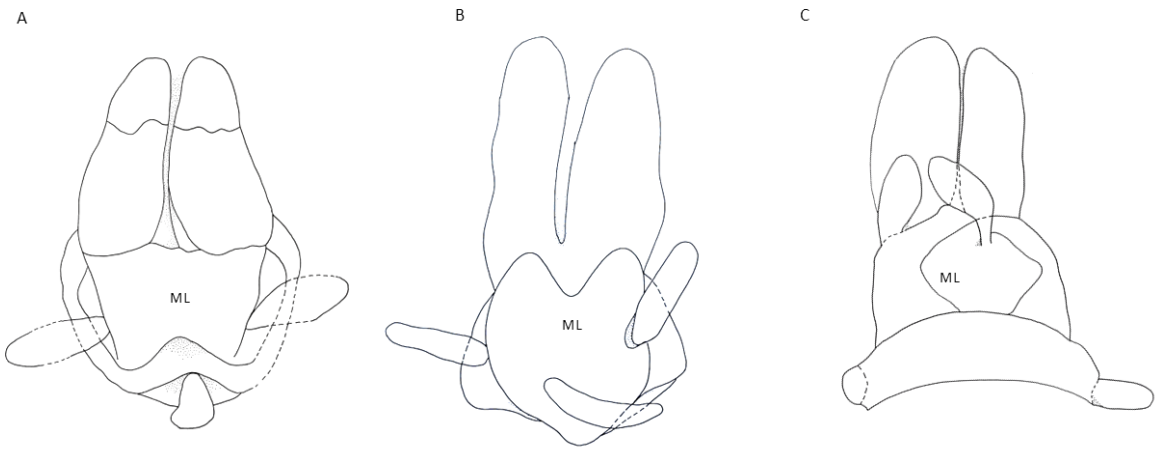

Fig. 6. Line drawings of prostomia of new species reported in this paper, with the shapes of median lobes (ML), drawings not to scale. **A**. *Anguillosyllis dalgleishae* sp. nov. **B**. *Anguillosyllis finnelli* sp. nov. **C**. *Anguillosyllis villarae* sp. nov.

P25593, *A. capensis* ZMH_P25594) and a maximum of 16 (*A. capensis* ZMH_P25588) mutations (1543 bp sequence).

Remarks

Morphologically, the new species can be distinguished from all other currently known species by the combination of the following characters: body with 10 chaetigers, presence of very large conical dorsal lobes (flaps) in parapodia and presence of dorsal cirri on chaetiger 1 only. *Anguillosyllis dalgleishae* sp. nov. can be distinguished from seven of the currently known species with 10 chaetigers by the presence of large parapodial dorsal lobes. Such lobes are currently known in only three species, that all possess 11, not 10 chaetigers: *A. palpata*, *A. hampsoni* and CCZ species *A. truebloodi*. Further, SEM confirmed the presence of dorsal cirri on chaetiger 1 only, a character currently confirmed by SEM only in other CCZ specimens assigned to *Anguillosyllis* cf. *hessleri* by Drennan *et al.* (2025). Maciolek (2020) using light microscopy considered such distribution as dorsal cirri "missing" in all but first segments.

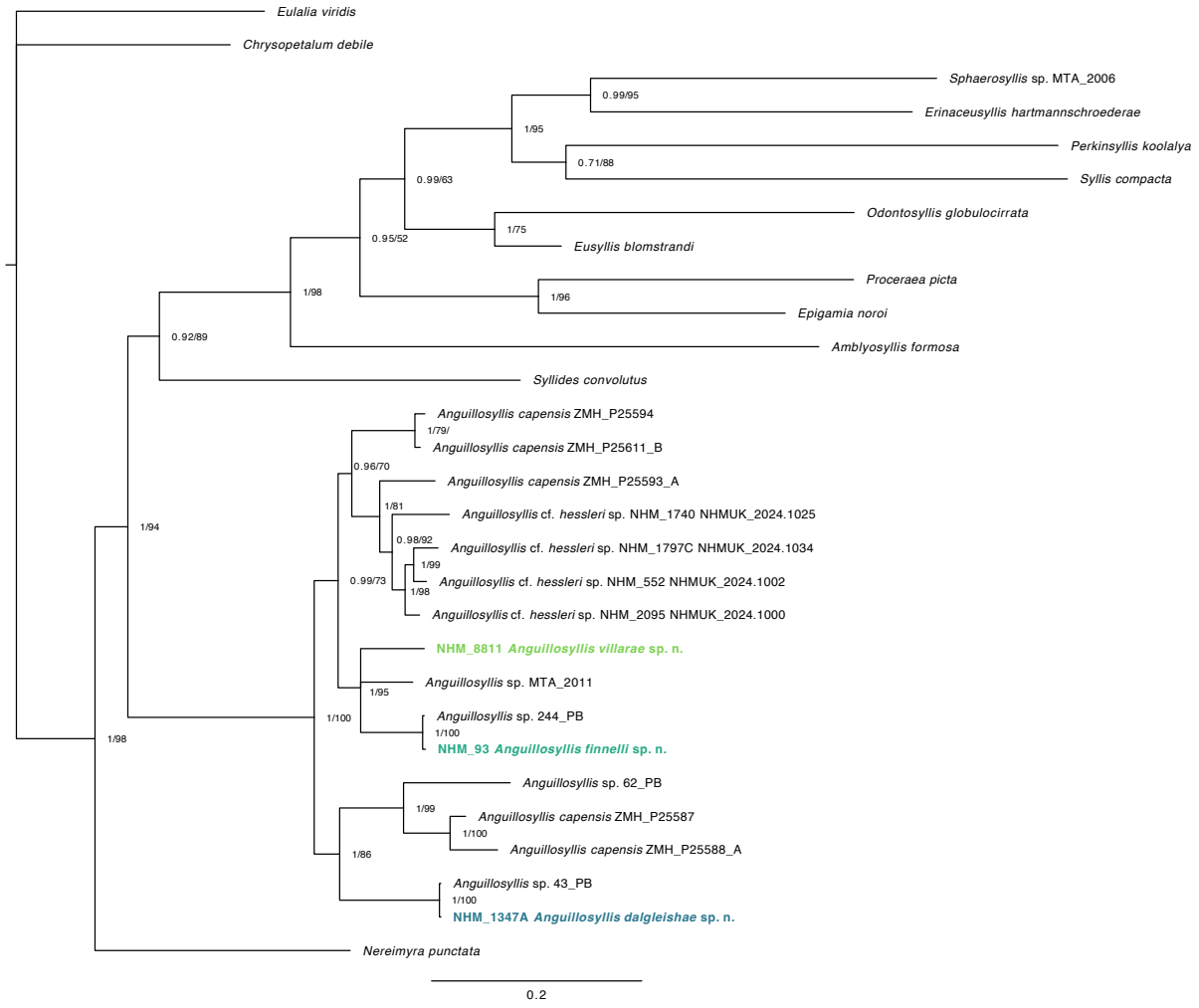

Fig. 7. Phylogenetic analysis of *Anguillosyllis* Day, 1963 using combined Bayesian analysis of three markers, cytochrome oxidase subunit I (COI), 16S RNA and 18S RNA. New species described in this study are highlighted in bold and colour. The tree also includes representatives of the *Anguillosyllis* cf. *hessleri* species complex described in Drennan *et al.* (2025), in addition to nine *Anguillosyllis*, ten syllid and three non-syllid nereidiform outgroup sequences from Genbank. Support values are given at nodes as Bayesian posterior probability values / maximum likelihood (ML) bootstrap values.

However, given our observations, it may be the case of true absence in the following 10 chaetigers bearing species: *A. taleola*, *A. sepula* and *A. elegantissima*.

Distribution

Eastern CCZ: UK-1 and OMS exploration areas, depth ~4200 m. Also, BGR area (Bonifácio *et al.* 2020).

Anguillosyllis finnelli sp. nov.
urn:lsid:zoobank.org:act:1E961327-01B3-4D90-8227-1C13C8756D03
Figs 6B, 8–12

Diagnosis

Body with 11 chaetigers. Prostomium in two parts, with three short antennae. Palps elongated, free to the base. Parapodia with large conical dorsal lobes (flaps). Dorsal cirri absent in chaetiger 2. Heterogomph chaetae unidentate.

Etymology

The species name is dedicated to Cletus Finnell, Able Seaman on the RV *Melville* on the October 2013 cruise 'ABYSSLINE AB01'.

Material examined

Holotype

PACIFIC OCEAN – **Eastern Central Pacific, Clarion Clipperton Fracture Zone** • 13.79335° N, 116.7030833° W; 4081 m depth; 11 Oct. 2013; A.G. Glover, H. Wiklund, T. Dahlgren and M. Georgieva leg.; USNEL Box Core; specimen GUID: 6d7ef8a1-9fa4-4eec-aca2-f68b1ace677b; field ID NHM_00093; GenBank COI gene: PV577530; 16S gene: PV579023; 18S gene: PV579030; NHMUK ANEA 2024.2720.

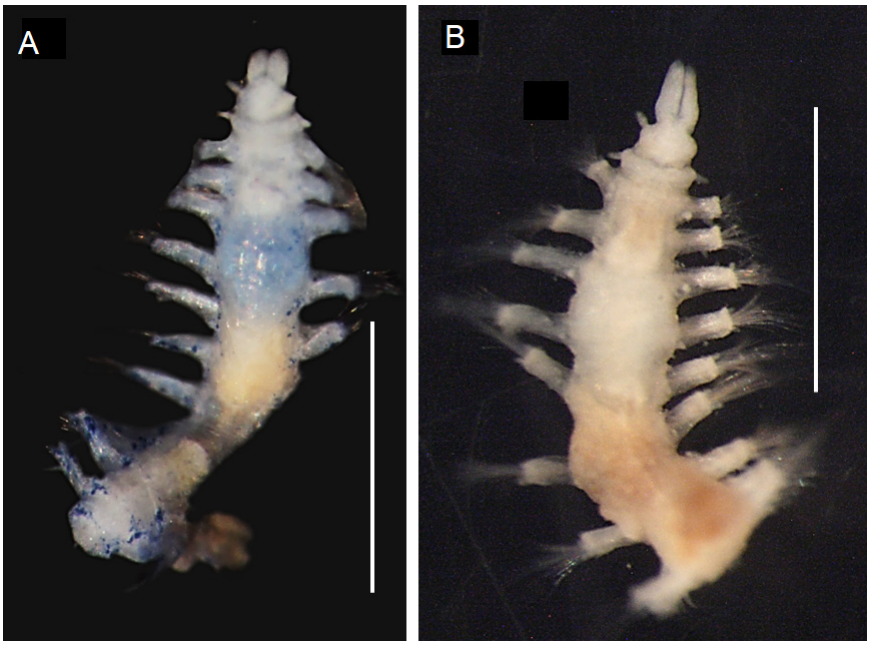

Fig. 8. *Anguillosyllis finnelli* sp. nov. **A**. Paratype (NHMUK ANEA 2024.2717), preserved, in dorsal view, with Shirlastain A residue. **B.** Preserved specimen (NHMUK ANEA 2024.2719) in dorsal view. Scale bars = 1 mm.

Paratypes

PACIFIC OCEAN – **Eastern Central Pacific, Clarion Clipperton Fracture Zone** • 1 spec.; 10.33079203° N, 117.1940202° W; 4290.89 m depth; 1 Jun. 2021; H. Wiklund, R. Drennan, C. Boolukos and G. Bribiesca Contreras leg.; USNEL Box Core; specimen GUID: c3b77851-d8d0-4a33-9f2b-2a993391f41d; field ID; NHM_08730A; GenBank COI gene: PV577528; NHMUK ANEA 2024.2717 • 1 spec.; 10.35561637° N, 117.1686897° W; 4280 m depth; 11 Nov. 2020; H. Wiklund, R. Drennan, C. Boolukos and G. Bribiesca Contreras leg.; USNEL Box Core; specimen GUID: 654e0cbb-ac72-4aec-93b0-a24302d3e16c; field ID NHM_05880; GenBank COI gene: PV664495; NHMUK ANEA 2024.2713.

Other material

PACIFIC OCEAN – **Eastern Central Pacific, Clarion Clipperton Fracture Zone** • 1 spec.; 12.36565642° N, 116.7520565° W; 4159.33 m depth; 10 Mar. 2020; A.G. Glover, H. Wiklund, G. Bribiesca Contreras and E. Simon Lledó leg.; USNEL Box Core; specimen GUID: 89b42808-8b28-431e-b4d1-7c7b486289b7; field ID NHM_04733_ECDS4; GenBank COI gene: PV577526; 16S gene: PV579021; NHMUK ANEA 2024.2714 • 1 spec.; 12.38927437° N, 116.6362959° W; 4179.39 m depth; 11 Mar. 2020; A.G. Glover, H. Wiklund, G. Bribiesca Contreras and E. Simon Lledó leg.; USNEL Box Core; specimen

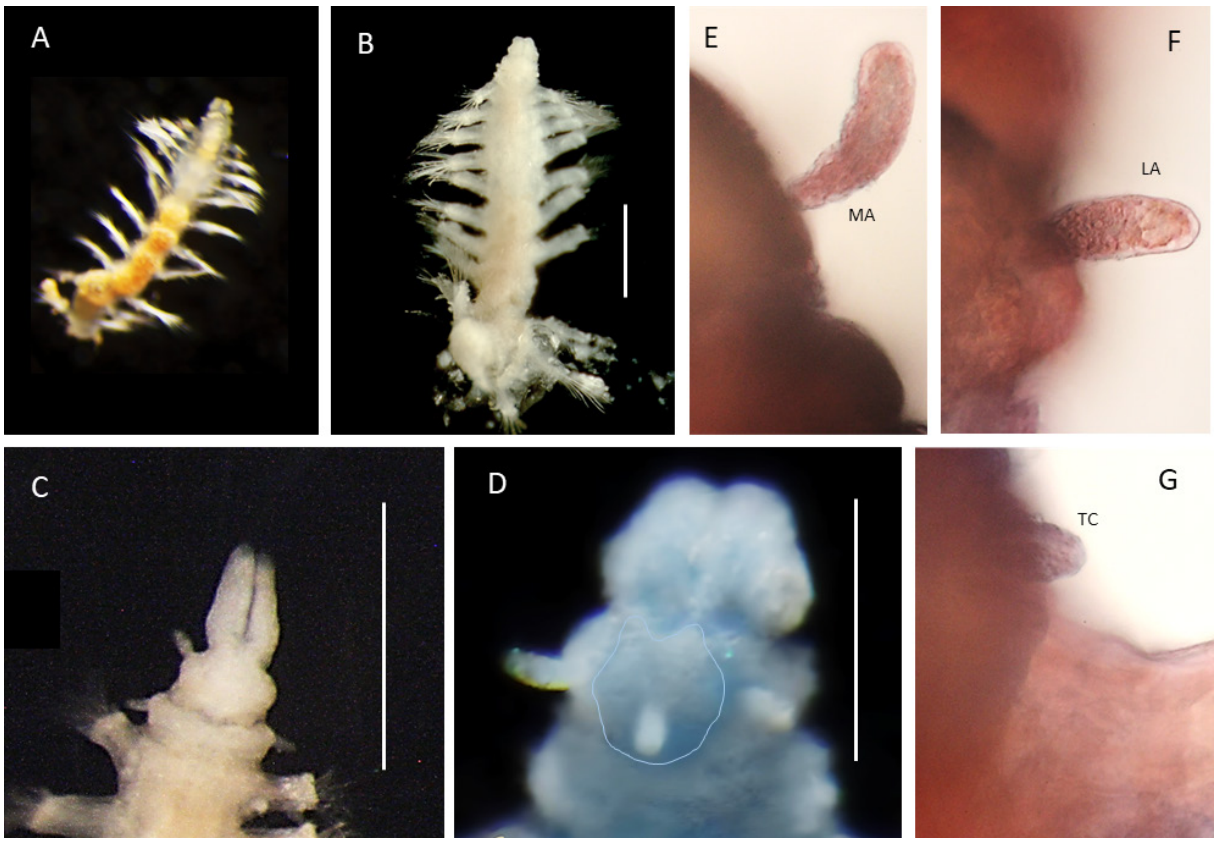

Fig. 9. *Anguillosyllis finnelli* sp. nov., holotype (NHMUK ANEA 2024.2720) unless stated otherwise; specimen stained with Shirlastain A in images D–G. **A**. Complete live specimen with 11 chaetigers in ventral view, image taken on board the ship. **B**. Now posteriorly incomplete preserved specimen in dorsal view, with tissue sampled for DNA. **C**. Fully extended palps in specimen NHMUK ANEA 2024.2719 in dorsal view. **D**. Detail of prostomium with outline of the median prostomial lobe traced by a thin line, palps curled ventrally, Shirlastain A faded. **E**. Detail of club-shaped median antenna (MA) in lateral view. **F**. Detail of lateral antennae (LA) in dorsal view. **G**. Tentacular cirrus (TC) in dorsal view. Scale bars = B–C = 500 µm; D = 250 µm.

GUID: c2db9a70-9ccb-4d7e-abbf-4bef0404844c; field ID NHM_04741_ECDS4; GenBank 16S gene: PV579022; NHMUK ANEA 2024.2715 • 1 spec.; 10.35780083° N, 117.1593114° W; 4284 m depth; 13 Nov. 2020; H. Wiklund, R. Drennan, C. Boolukos and G. Bribiesca Contreras leg.; USNEL Box Core; specimen GUID: 68b5e2d7-8061-4f19-adad-b577c49fb335; field ID NHM_08783_HW01; GenBank COI gene: PV577529; NHMUK ANEA 2024.2718 • 1 spec.; 10.33498329° N, 117.1741855° W; 4286 m depth; 6 Nov. 2020; H. Wiklund, R. Drennan, C. Boolukos and G. Bribiesca Contreras leg.; USNEL Box Core; specimen GUID: 8a93a352-604b-420f-b328-930c84d540cf; field ID NHM_08789_HW05; GenBank COI gene: PV664496; NHMUK ANEA 2024.2719 • 1 spec.; 10.35561637° N, 117.1686897° W; 4280 m depth; 11 Nov. 2020; H. Wiklund, R. Drennan, C. Boolukos and G. Bribiesca Contreras leg.; USNEL Box Core; specimen GUID: 04898df3-ab82-4b5d-8c82-7f0a5a396eac; field ID NHM_08801_HW03; GenBank COI gene: PV577527; NHMUK ANEA 2024.2716 • 1 spec.; 10.333014° N, 117.18551° W; 4281 m depth; 12 Feb. 2022; H. Wiklund, C. Boolukos, E. Stewart and A. Bessell leg.; USNEL Box Core; specimen GUID: 15c30fcb-cfdb-46c1-9066-f6eb52c4eb09; field ID NHM_10334_CB3; GenBank COI gene: PV577532; NHMUK ANEA 2024.2722 • 1 spec.; 10.353342° N, 117.242837° W; 4296 m depth; 19 Nov. 2022; H. Wiklund, C. Boolukos, E. Stewart and A. Bessell leg.; USNEL Box Core; specimen GUID: 1cd18a15-4081-482f-b380-418cbe9a20e9; field ID NHM_10372_CB06; GenBank COI gene: PV664497; NHMUK ANEA 2024.2723 • 1 spec.; 13.7309° N, 126.2041° W; 4704 m depth; 20 Feb. 2023; A.G. Glover, E. Stewart, G. Bribiesca Contreras and E. Simon Lledó leg.; USNEL Box Core; specimen GUID: f7d6faae-4c53-4fcd-a168-e55f53d3201c; field ID NHM_10602_GB01; GenBank COI gene: PV577531; NHMUK ANEA 2024.2721.

Description

Measurements and appearance. Moderately sized species, up to 2 mm in length for 11 chaetigers (Fig. 8A–B). Holotype NHMUK ANEA 2024.2720, now posteriorly incomplete due to tissue sampling

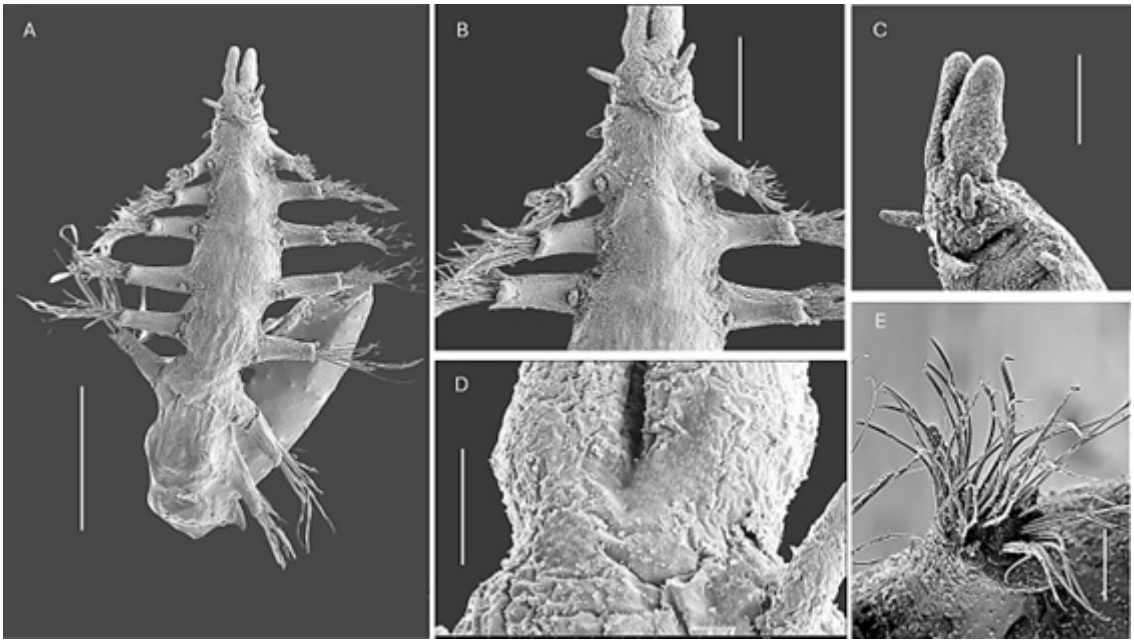

Fig. 10. *Anguillosyllis finnelli* sp. nov., paratype (NHMUK ANEA 2024.2713), SEM micrographs. **A**. Posteriorly incomplete specimen in dorsal view. **B**. Anterior end in dorsal view, with detail of prostomium and dorsal cirrophores on chaetigers 1 and 3, showing true absence on chaetiger 2. **C**. Detail of prostomium and palps in lateral view. **D**. Detail of attachment of palps to prostomium, showing palps free to the base. **E.** Bundle of chaetae from anterior parapodium. Scale bars: A = 500 μm; B = 200 μm; C = 100 μm; D–E = 50 μm.

for DNA, ~1.65 mm long and 0.25 mm wide for 7 chaetigers (Fig. 9A, C); live specimen presented with complete body with 11 chaetigers (Fig. 9A). Paratype NHMUK ANEA 2024.2717, now posteriorly incomplete with 9 chaetigers, 1.8 mm long and 0.3 mm wide at widest point (Fig. 8B). Paratype NHMUK ANEA 2024.2713, SEM specimen on stub, posteriorly incomplete and damaged, ~1.55 mm long and 0.25 mm wide for 7 chaetigers (Fig. 10A). Other specimens in variable condition, usually posteriorly incomplete due to fragmentation or tissue sampling for DNA, where complete body with 11 chaetigers. Body somewhat dorsoventrally flattened, tapering slightly from chaetiger 4 anteriorly. Live specimen semi-translucent, without pigmentation (Fig. 9A); fixed specimen opaque, creamy white to pale yellow in ethanol (Figs 8A–B, 9B).

Prostomium. Oval, wider than long; differentiation of median lobe visible even under light microscopy in holotype (Fig. 9D); median lobe broadly pentagonal, anteriorly with two broad peaks (Figs 6B, 9D). Eyes absent. Prostomium bearing three short, digitiform to club-shaped antennae and two palps (Figs 9E–F, 10A–C). Antennae slightly shorter than the prostomium; median antenna club shaped (Fig. 9E), slightly longer than lateral antennae, and inserted posterio-dorsally on the prostomium; lateral antennae digitiform (Fig. 9F), inserted more anteriorly. Palps ~1.5 the length of prostomium, digitiform, thick and distally rounded, free to the base when fully extended (Figs 9C, 10A–D); curled ventrally in holotype, obscuring their true shape (Fig. 9A–B, D).

Tentacular segment. Achaetous, bearing two, very short, papilliform tentacular cirri, >⅓ the length of the antennae and inserted laterally (Figs 9G, 10B). Pharyngeal tube extending to chaetiger 3, unarmed; proventricle spanning from chaetigers 3–5, barrel-shaped; number of muscle cell rows mostly obscured by body wall in preserved specimens, best observed in live specimen (Fig. 9A).

Parapodia. Long, rectangular, and uniramous. Parapodia with distally rounded, large conical dorsal lobe (Figs 10A–B, 11A) and two short papilliform lobes with anterior and posterior lobes of similar

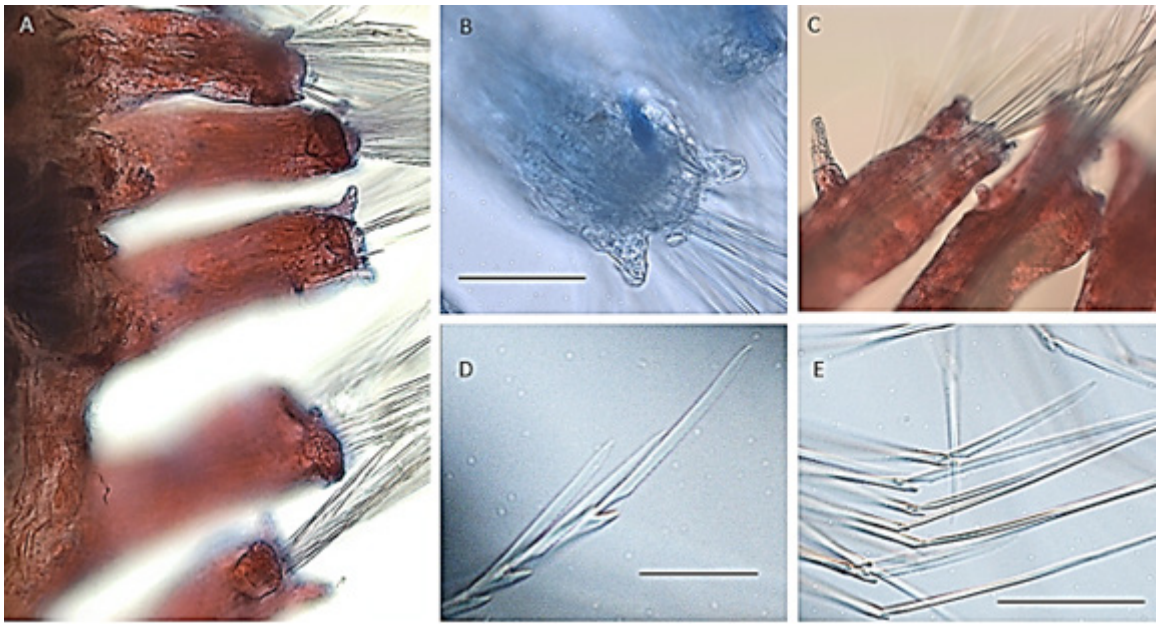

Fig. 11. *Anguillosyllis finnelli* sp. nov., holotype (NHMUK ANEA 2024.2720) stained with Shirlastain A. **A**. Parapodia with parapodial lobes. **B**. Detail of parapodial lobes. **C**. Parapodium with ventral cirrus. **D**. Compound chaetae from chaetiger 2. **E**. Compound chaetae from chaetiger 4. Scale bars: B = 25 µm; D–E = 50 µm.

size (Fig. 11B). Dorsal cirri missing, SEM shows presence of cirrophores on all chaetigers, except for chaetiger 2 where truly absent (Fig. 10A–B). Ventral cirri conical, and short approximately half the length of the antennae, inserted midway to ⅔ along the length of the parapodia moving away from the body (Fig. 11C). At least three acicula per parapodium, two with emergent tips. Each parapodium bearing dense bundles of numerous compound heterogomph chaetae (Fig. 11A), with chaetal bundles becoming somewhat sparser posteriorly. Anterior falcigerous chaetae with denticulated shafts, denticles arranged in irregular horizontal rows (Fig. 12A); other chaetae with smooth shafts and finely serrated, unidentate blades decreasing in length dorso-ventrally, ranging from elongate, slender spiniger-like to shorter falcigers (Figs 11D–E, 12B–C). Blades of the longest spiniger-like chaetae ~170 µm, and shortest falcigers ~20 µm. Tips of compound chaetae blunt, unidentate, at most gently hooked (Fig. 12B–C).

Pygidium. Damaged; pygidial appendages missing.

Genetic data

Specimens (n = 11) assigned to *A. finnelli* sp. nov. form a clade (Supp. file 3: Fig. S1, Supp. file 4: Fig. S2), with low intraspecific divergence across all sequences (maximum intraspecific p-distance/K2P distance 0.5/0.5% for 16S and 1.9/1.9% for COI). Sequences matched with high % identity (99–100%) in blastn search and by intraspecific distance (maximum p-distance/K2P 1.8/1.8%) to a COI sequence of an unidentified *Anguillosyllis* specimen (accession number: MK971075; ID: *Anguillosyllis* sp. 244_PB voucher 088-IOM-0246) (Fig. 7) collected from the IOM contract area of the Eastern CCZ, published in Bonifácio *et al.* (2020). In combined analyses (Fig. 7), this species is close to a polytomy consisting of *Anguillosyllis villarae* sp. nov. and GenBank sequences identified as *Anguillosyllis* sp. MTA_2011 from Costa Rica (accession numbers 18S:JF903571; 16S: JF903680; COI: JF903756) published in Aguado *et al*. (2012). However, minimum interspecific p-distance/K2P of 14.4/16% 16S, and 16.1/18.3% COI were observed between these species and *A. finnelli*, while in an alignment of nuclear 18S (1630 bp),

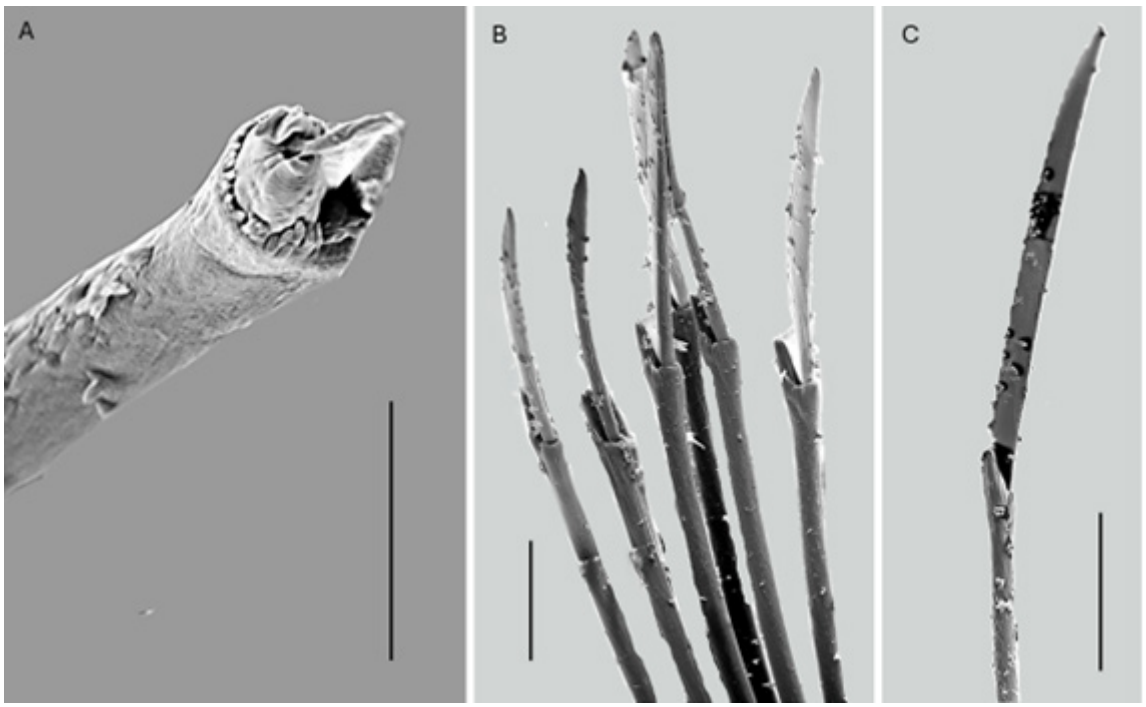

Fig. 12. *Anguillosyllis finnelli* sp. nov., paratype (NHMUK ANEA 2024.2713), SEM micrographs. **A**. Falcigerous chaetae of chaetiger 3 with denticulated ornamented shafts. **B**. Falcigerous chaetae from chaetiger 1. **C**. Chaeta from chaetiger 2. Scale bars: A = 5 µm; B = 10 µm; C = 20 µm.

A. finnelli differed by two and four mutations from *A. villarae* sp. nov and *Anguillosyllis* sp. MTA_2011 respectively.

Remarks

The new species belongs to the group of *Anguillosyllis* with 11 chaetigers, well-developed parapodial lobes and palps free to a large extent, although this character is difficult to establish when palps are curled up (Neal pers. obs.). Of the known species, *Anguillosyllis truebloodi* also shares such characters, and also the CCZ distribution (DOMES site, Wilson 2017). However, the new species can be easily distinguished by the true absence of dorsal cirri on chaetiger 2 as revealed by SEM (Fig. 10B), which is present in *A. truebloodi*. Maciolek (2020) also reported palps as fused halfway to the base in *A. truebloodi*, whilst these are free to the base in the new species (Fig. 10A, D), although from certain angles, particularly where bent, the palps may appear fused. Another similar species is *Anguillosyllis palpata* with type locality in the Drake Passage in relatively shallow depths of 384–494 m, which has since been widely reported worldwide, including abyssal depths (Maciolek 2020). Morphological variation in specimens identified as *A. palpata* has been reported by Maciolek (2020), but in the absence of molecular data, species differentiation is difficult. The species newly reported here differs from *A. palpata* in the form of the chaetae, which are distinctly hooked in *A. palpata*, but not in the new species, in which they are at most gently hooked (Figs 11D, 12B–C), absence of large postchaetal lobes and true absence of dorsal cirri on chaetiger 2 (Fig. 10B).

Distribution

Eastern CCZ: NORI-D exploration area, depth ~4300 m; UK-1 exploration area, depth ~4200 m; OMCO site, depth ~4700 m. Also, IOM area (Bonifácio *et al.* 2020).

Anguillosyllis villarae sp. nov.
urn:lsid:zoobank.org:act:E0177D9E-D221-48C7-A76C-2804FD4C469C
Figs 6C, 13–16

Diagnosis

Body with 10 chaetigers. Prostomium in two parts, with three short antennae. Palps elongated, free to the base. Parapodia with large conical dorsal lobes (flaps). Heterogomph chaetae unidentate with some tips hooked or with tips bidentate; some chaetae with wide strap-like blades.

Etymology

The species name is dedicated to Lucía Villar Muñoz a member of the science party on expeditions C5a, C5d, C7a, and C7b to the NORI-D area, particularly for her work slicing and sieving boxcore samples.

Material examined

Holotype

PACIFIC OCEAN – **Eastern Central Pacific, Clarion Clipperton Fracture Zone** • 10.354901° N, 117.220794° W; 4273.8 m depth; 23 Nov. 2020; H. Wiklund, R. Drennan, C. Boolukos and G. Bribiesca Contreras leg.; USNEL Box Core; specimen GUID: aa8735af-ee3a-456f-bc57-888dd874e7fc; field ID; NHM_08811; GenBank COI gene: PV577536; 16S gene: PV579024; 18S gene: PV579032; NHMUK ANEA 2024.2704.

Paratypes

PACIFIC OCEAN – **Eastern Central Pacific, Clarion Clipperton Fracture Zone** • 1 spec.; 10.32909125° N, 117.1971482° W; 4281 m depth; 9 Nov. 2020; H. Wiklund, R. Drennan, C. Boolukos and G. Bribiesca Contreras leg.; USNEL Box Core; specimen GUID: c382ab84-7641-40bb-91db-

107aa41c8eee; field ID NHM_05657; GenBank COI gene: PV577533; NHMUK ANEA 2024.2701 • 1 spec.; 10.34811115° N, 117.1706608° W; 4282.6 m depth; 17 May. 2021; H. Wiklund, R. Drennan, C. Boolukos and G. Bribiesca Contreras leg.; USNEL Box Core; specimen GUID: 2280eace-04fb-430a-aa3f-d2163f629c86; field ID NHM_07689B; GenBank COI gene: PV577537; NHMUK ANEA 2024.2706.

Other material

PACIFIC OCEAN – **Eastern Central Pacific, Clarion Clipperton Fracture Zone** • 1 spec.; 10.33498329° N, 117.1741855° W; 4286 m depth; 6 Nov. 2020; H. Wiklund, R. Drennan, C. Boolukos and G. Bribiesca Contreras leg.; USNEL Box Core; specimen GUID: 8a50f3cb-93de-4aa6-8792-cac45d2b2137; field ID NHM_05399; GenBank 16S gene: PV579028; NHMUK ANEA 2024.2712 • 1 spec.; 10.3861134° N, 117.1309018° W; 4308 m depth; 12 Nov. 2020; H. Wiklund, R. Drennan, C. Boolukos and G. Bribiesca Contreras leg.; USNEL Box Core; specimen GUID: bc633595-9ba5-4320-a0c8-e0022060eac7; field ID NHM_05908; GenBank 16S gene: PV579025; NHMUK ANEA 2024.2705 • 1 spec.; 10.33426964° N, 117.1901234° W; 4287.72 m depth; 12 May. 2021; H. Wiklund, C. Boolukos, M. Rabone and G. Bribiesca-Contreras leg.; USNEL Box Core; specimen GUID: 50527b56-3f4d-430f-929b-fa4d91b1d858; field ID NHM_06940; GenBank 16S gene: PV579027; NHMUK ANEA 2024.2711 • 1 spec.; 10.37726533° N, 117.1558078° W; 4302.03 m depth; 14 May. 2021; H. Wiklund, C. Boolukos, M. Rabone and G. Bribiesca Contreras leg.; USNEL Box Core; specimen GUID: 45112357-3af9-4c7f-8c93-d014c68f64ca; field ID NHM_07227A; GenBank 16S gene: PV579026; NHMUK ANEA 2024.2710 • 1 spec.; 10.33079203° N, 117.1940202° W; 4290.89 m depth; 1 Jun. 2021; H. Wiklund, R. Drennan, C. Boolukos and G. Bribiesca Contreras leg.; USNEL Box Core; specimen GUID: 71da1d0f-f4b9-4390-a8de-4c55e8351ad0; field ID NHM_08730; GenBank COI gene: PV577534; NHMUK ANEA 2024.2702 • 1 spec.; 10.33079203° N, 117.1940202° W; 4290.89 m depth; 1 Jun. 2021; H. Wiklund, R. Drennan, C. Boolukos and G. Bribiesca Contreras leg.; USNEL Box Core; specimen GUID: 290627ed-657b-4965-a9bd-920e8ca878ce; field ID NHM_08730B; GenBank COI gene: PV577535; 18S gene: PV579031; NHMUK ANEA 2024.2703 • 1 spec.; 10.332533° N, 117.187352° W; 4281 m depth; 24 Aug. 2022; H. Wiklund, C. Boolukos and E. Stewart leg.; USNEL Box Core; specimen GUID: d38da487-db2d-4274-bc96-ba7af0112e02; field ID NHM_09396_HW18; GenBank COI gene: PV577538; NHMUK ANEA 2024.2707 • 1 spec.; 10.334243° N, 117.185992° W; 4279 m depth; 12 Mar. 2022; H. Wiklund, C. Boolukos, E. Stewart and A. Bessell leg.; USNEL Box Core; specimen GUID: 82b4921b-0ff9-4337-9bc4-034367e808c5; field ID NHM_10276; GenBank COI gene: PV577539; NHMUK ANEA 2024.2708 • 1 spec.; 10.334296° N, 117.17708° W; 4282 m depth; 21 Nov. 2022; H. Wiklund, C. Boolukos, E. Stewart and A. Bessell leg.; USNEL Box Core; specimen GUID: fe6b7444-31bf-400f-9ed1-66530bb53a8c; field ID NHM_10374_CB12 ; GenBank COI gene: PV577540; NHMUK ANEA 2024.2709.

Description

Measurements and appearance. Moderately sized species, up to 2 mm in length for 10 chaetigers (Fig. 13A–C). Holotype NHMUK ANEA 2024.2704, posteriorly complete, 1.6 mm long and 0.25 mm at widest point for 10 chaetigers; only left lateral antenna remains attached, pygidium with cirri missing (Fig. 13A–B). Paratype NHMUK ANEA 2024.2701, live specimen translucent with 10 chaetigers (Fig. 13C), now as SEM specimen on stub, posteriorly incomplete, ~0.8 mm long and 0. 25 mm wide at widest point for 5 chaetigers, left lateral antenna missing (Fig. 14A). Paratype NHMUK ANEA 2024.2706, specimen with 10 chaetigers, with pygidium removed for tissue sampling for DNA analysis, rest of the body well preserved, ~1.3 mm long 0.25 mm wide. Other specimens in variable condition, usually posteriorly incomplete due to preservation or tissue sampling for DNA. Body somewhat dorsoventrally flattened. Fixed specimen opaque, creamy white in ethanol (Fig. 13 A–B).

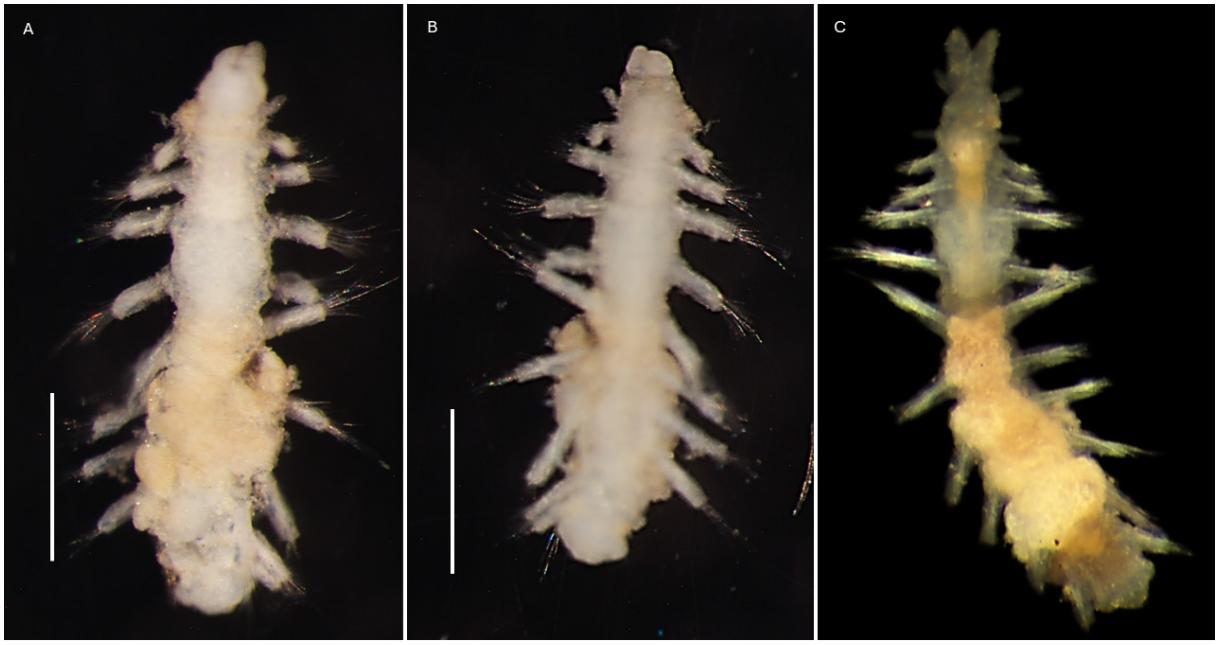

Fig. 13. *Anguillosyllis villarae* sp. nov. **A–B**. Holotype (NHMUK ANEA 2024.2704). **A**. Complete specimen in dorsal view. **B**. Complete specimen in ventral view. **C**. Paratype (NHMUK ANEA 2024.2701), live specimen in dorsal view. Scale bars = 500 µm.

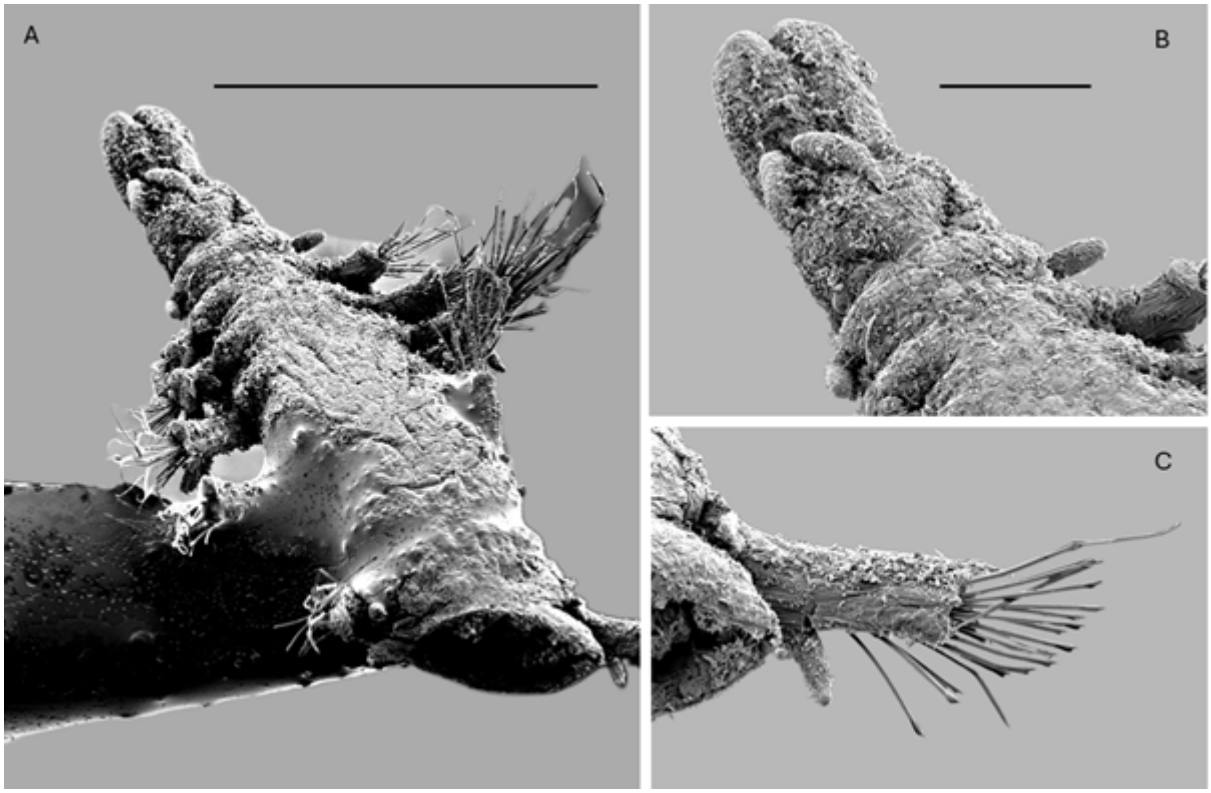

Fig. 14. *Anguillosyllis villarae* sp. nov., paratype (NHMUK ANEA 2024.2701), SEM micrographs. **A**. Posteriorly incomplete specimen in postero-dorsal view. **B**. Detail of anterior end in postero-dorsal view. **C**. 5th parapodium with ventral cirrus. Scale bars: A = 500 µm; B = 100 µm.

Prostomium. Oval, wider than long (Fig. 13A) under light microscope; SEM shows differentiation with distinct median lobe approximating the diamond shape in postero-dorsal view (Figs 6C, 14B). Eyes absent. Prostomium bearing three short digitiform to club-shaped antennae and two palps (Fig. 14A–B). Antennae about the length of prostomium; median antenna club shaped, slightly longer than lateral antennae, and inserted on the prostomial median lobe (Fig. 14A–B); lateral antennae digitiform, inserted more anteriorly on the inferior prostomial lobe (Fig. 14A–B). Palps slightly longer than the prostomium, thick, digitiform and distally rounded, free to the base (Fig. 14A–B).

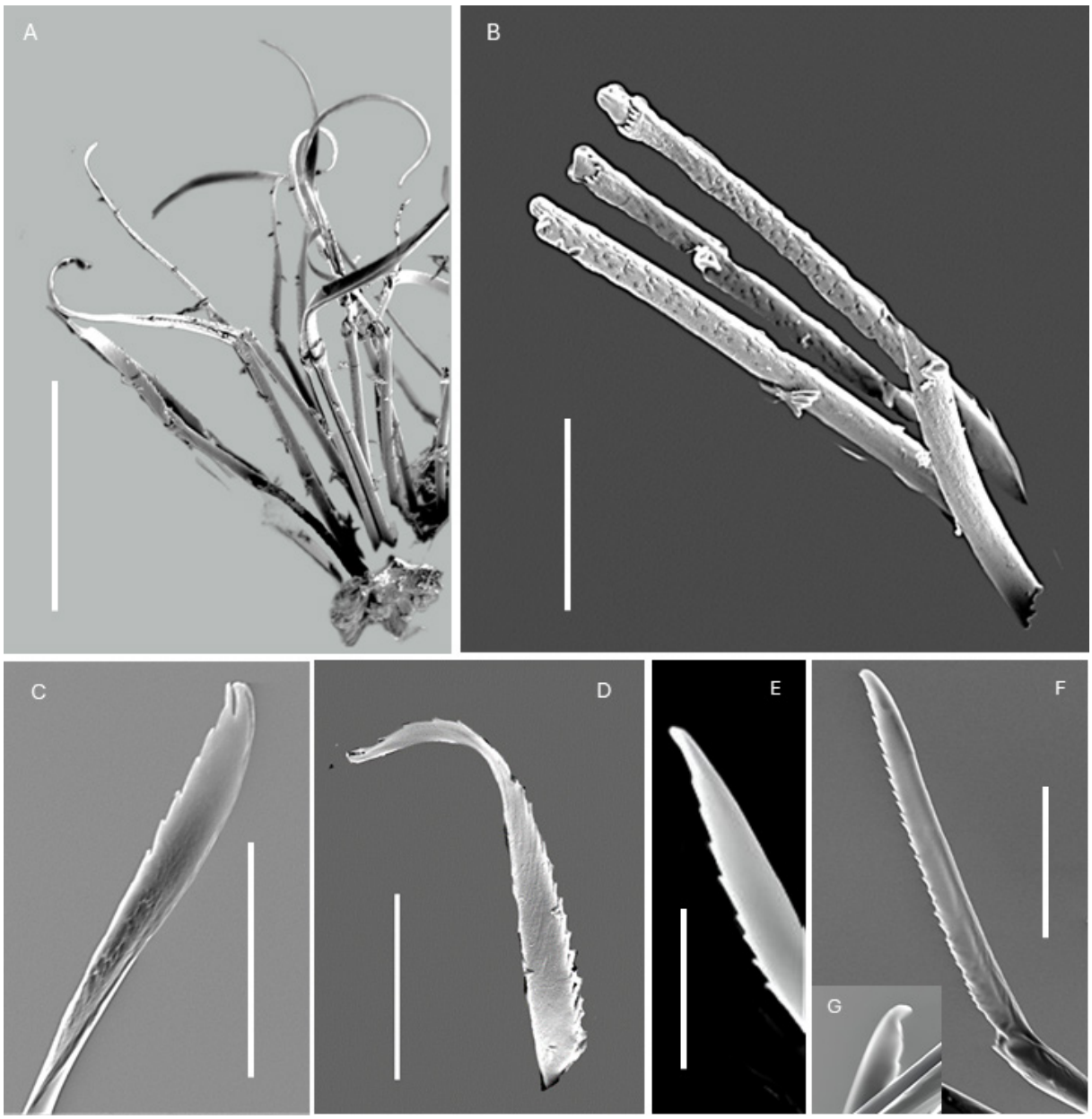

Fig. 15. *Anguillosyllis villarae* sp. nov., paratype (NHMUK ANEA 2024.2701), SEM micrographs. **A**. Bundle of chaetae from anterior chaetiger. **B**. Denticulated chaetal shafts from falcigers of chaetiger 1. **C**. Bidentate falciger. **D**. Falciger with broad, densely serrated blade. **E**. Falciger with narrow tip. **F**. Falciger with blunt tip. **G**. Falciger with hooked tip. Scale bars: A = 50 µm; B, D, F = 10 µm; C, E = 5 µm.

Tentacular segment. Achaetous, bearing two short oval tentacular cirri, ~½ the length of median antenna, inserted laterally (Fig. 14A–B). Pharyngeal tube extending to chaetiger 3; proventricle spanning from chaetigers 3–5 lightbulb shaped; number of muscle cell rows mostly obscured by body wall.

Parapodia. Long, rectangular, and uniramous. Parapodia with well-developed conical dorsal lobe and two smaller lobes, best observed in paratype NHMUK 2024.2706 (Fig. 16A–B). Internal glands in the distal part of parapodia retain Shirlastain A. Dorsal cirri always missing, SEM shows presence of cirrophores on chaetiger 1, unclear in other chaetigers. Ventral cirri short and conical, approximately half the length of the antennae, inserted medially on parapodia (Fig. 14C). Only one aciculum per parapodium confirmed, with non-emergent tip (Fig. 16C). Each parapodium with sparse bundles of ~15–20 chaetae. All chaetae compound heterogomph, falcigerous to spiniger-like (Fig. 16D–E). Shafts of falcigerous chaetae in chaetigers 1–4 denticulated with denticles arranged in irregular horizontal rows (Fig. 15B), other shafts smooth. Blades variable ranging from sturdy and thin with sparse serration to wide, strap-like, 'floppy' and densely serrated chaetae, best observed in mid body parapodia (Fig. 15A, D). Tips of chaetae blunt, unidentate gently curved (Fig. 15E–F) or distinctly hooked (Fig. 15G), some tips distinctly bidentate (Fig. 15C).

Pygidium. Damaged; pygidial appendages missing.

Genetic data

Specimens (n = 12) assigned to *A. villarae* sp. nov. form a monophyletic clade (Supp. file 3: Fig. S1, Supp. file 4: Fig. S2), with low intraspecific divergence across all sequences (maximum intraspecific

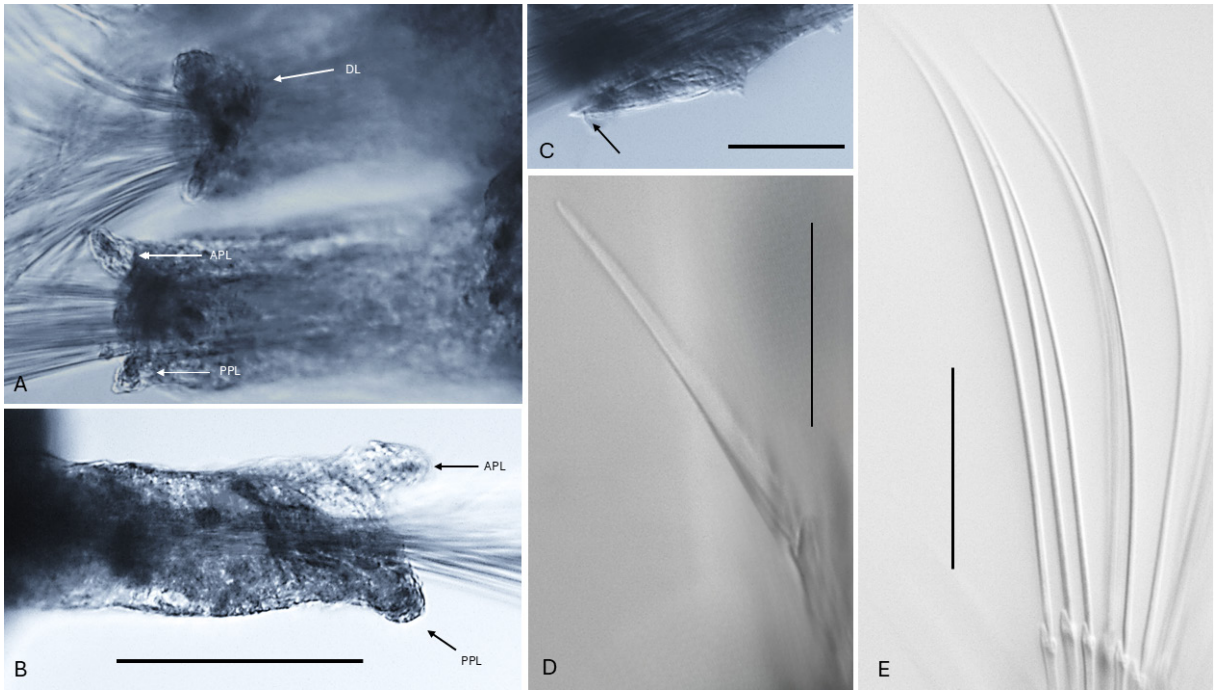

Fig. 16. *Anguillosyllis villarae* sp. nov., paratype (NHMUK ANEA 2024.2706). **A**. Midbody parapodia, showing parapodial lobes (marked by arrows. **B**. Detail of 7th parapodium with parapodial lobes. **C**. Parapodium showing non-emergent aciculum (marked by arrow). **D**. Falcigerous chaeta as seen under light microscope. **E**. Slender spiniger-like chaetae as seen under light microscopy. Abbreviations: APL = anterior parapodial lobe; DL = dorsal lobe; PPL = posterior parapodial lobe. Scale bars: B = 125 µm; C–E = 50 µm.

p-distance/K2P 0.8/0.8% for 16S and 0.5/0.5% for COI). No close matches on GenBank were returned following blastn analysis. In the combined phylogenetic analysis (Fig. 6), this species forms a polytomy with sequences identified as *Anguillosyllis* sp. MTA_2011 (discussed in *A. finnelli* genetics section) in addition to being close to *Anguillosyllis finnelli* sp. nov. In separate gene analyses (Supp. file 3: Fig. S1, Supp. file 4: Fig. S2), minimum interspecific p-distances/K2P of 13.4/14.8% 16S, and 17.1/19.5% COI were observed between *A. villarae* and *A. finnelli*, and 12.3/13.2% 16S and 19.3/26.6% COI between *A. villarae* and *Anguillosyllis* sp. MTA_2011. *Anguillosyllis villarae* differed from *A. finnelli* and *Anguillosyllis* sp. MTA_2011 by two and six mutations respectively in an alignment of nuclear 18S (1630 bp).

Remarks

The new species described here is easily distinguished from most known species, by the presence of hooked and bidentate chaetae. Currently only three known species, *Anguillosyllis palpata*, *A. hampsoni* and *A. truebloodi* (CCZ species), possess hooked chaetae. However, only in the new species described here, we have observed distinctly bidentate tips (Fig. 15C). Another character shared with *A. palpata* is the presence of well-developed dorsal lobes in parapodia. However, all known species that possess the enlarged dorsal lobe have a body with 11 chaetigers, while the new species has only 10. The prostomium of the new species cannot be meaningfully compared as no SEM investigations have been published previously, but it possesses a distinct median lobe approximating the diamond shape (Fig. 14B) at least when observed postero-dorsally.

Distribution

Eastern CCZ: NORI-D exploration area, depth ~4300 m.

Discussion

Recent taxonomic work revealed a great species richness of *Anguillosyllis*, with 16 species newly described from worldwide deep-sea locations (Maciolek 2020), bringing the number of currently valid species to 20. This study has added three formally described species of *Anguillosyllis* from 37 specimens to the knowledge of annelid biodiversity within investigated areas of the eastern CCZ (see Rabone *et al.* 2023a). In total, we have now identified 68 annelid species from the areas targeted by this study, with 21 of them formalised (Wiklund *et al.* 2019; Drennan *et al.* 2021; Neal *et al.* 2022a, 2022b, 2023; this study), with further 129 informal annelid species names, published as records only (Wiklund *et al.* 2023).

In terms of *Anguillosyllis* diversity, this study brings the number of formally described species worldwide to 23 and within the CCZ to five, with many more species likely to be discovered within the deep-sea. As supported by recent molecular work (Drennan *et al.* 2025), the genetic diversity of this genus within the CCZ may be greater than previously thought. High genetic diversity may not be restricted to the CCZ. Sequences from specimens morphologically identified as *Anguillosyllis capensis* collected from abyssal waters in the Southeastern Atlantic in Böggemann (2009) were polyphyletic across the combined phylogenetic analyses in this study, with at least three separate lineages (Fig. 7). This high diversity was also shown in Böggemann (2009) across both mitochondrial and nuclear genes. Due to the geographic, and even more importantly, bathymetric distances between the type locality (off South Africa, 183 m) and abyssal SE Atlantic sites (3950–5655 m depth), it is possible that none of the lineages in Böggemann (2009) represent the 'true' *A. capensis*, as already suggested by Maciolek (2020). However, no molecular data are available from the type material or the type locality for comparison.

Discovery of such diversity suggests that sole reliance on morphological characters obtained by light microscopy is insufficient to detect the true diversity in this genus. We would therefore caution against further formalisations of new species of *Anguillosyllis* without an integrative approach also using genetic

data, and other morphological data such as those obtained from SEM observations. We particularly recommend further examination of characters such as prostomial lobes and absence of dorsal cirri along the body. The taxonomic reliability of those characters warrants further investigation. The lack of knowledge of such characters in previously described species hampers meaningful morphological comparisons and, in some cases, prevents the formalisation of new species. This poses significant consequences for any conservation efforts across the CCZ as the biodiversity and geographical ranges of *Anguillosyllis* species cannot be determined without the ability to correctly identify the species.

Acknowledgements

We thank the masters, crew, and technical staff on the vessels mentioned above for their outstanding support. We acknowledge the expert leadership of the ABYSSLINE project by Prof. Craig R Smith, University of Hawaii. We received help sorting and sieving samples at sea from science teams in successful deep-sea coring operations on all cruises. We acknowledge the #NHMDeepSea Project Manager Dr Georgina Glaser for assistance throughout as well as the continued support from the NHMUK Consultancy team (Harry Rousham, Robyn Fryer, Kate Rowland, Joshua Herrington). We acknowledge the assistance of Zuzana Jungmanová with the completion of Figure 6. This research was supported by funding from UK Seabed Resources Ltd, The Metals Company and Natural Environment Research Council grant 'SMARTEX – Seabed Mining and Resilience to Experimental Impact' grant NE/T002913/1. Adrian G. Glover and Thomas D. Dahlgren have received support from TMC Inc. (The Metals Company) through its subsidiary Nauru Ocean Resources Inc. (NORI). NORI holds exploration rights to the NORI-D contract area in the CCZ regulated by the International Seabed Authority and sponsored by the government of Nauru. This is contribution TMC/NORI/D/025. We also acknowledge the continued support of UK Seabed Resources for funding the fundamental taxonomic studies necessary to inform the regulation of potential industrial activity. This research was also supported by funding from Norwegian Research Council (JPIOceans Mining Impact II).

References

Aguado M.T. & San Martín G. 2008. Re-description of some enigmatic genera of Syllidae (Phyllodocida: Polychaeta). *Journal of the Marine Biological Association of the United Kingdom* 88 (1): 35–56. https://doi.org/10.1017/S002531540800026X

Aguado M.T. & San Martín G. 2009. Phylogeny of Syllidae (Annelida, Phyllodocida) based on morphological data. *Zoologica Scripta* 38 (4): 379–402. https://doi.org/10.1111/j.1463-6409.2008.00380.x

Aguado M.T., San Martín G. & Siddall M.E. 2012. Systematics and evolution of syllids (Annelida, Syllidae). *Cladistics* 28 (3): 234–250. https://doi.org/10.1111/j.1096-0031.2011.00377.x

Barroso R., Paiva P.C., Nogueira J.M.M. & Fukuda M.V. 2017. Deep sea Syllidae (Annelida, Phyllodocida) from Southwestern Atlantic. *Zootaxa* 4221 (4): 401–430. https://doi.org/10.11646/zootaxa.4221.4.1

Bely A.E. & Wray G.A. 2004. Molecular phylogeny of naidid worms (Annelida: Clitellata) based on cytochrome oxidase I. *Molecular Phylogenetics and Evolution* 30 (1): 50–63. https://doi.org/10.1016/S1055-7903(03)00180-5

Blake J.A. 2019. New species of Cirratulidae (Annelida, Polychaeta) from abyssal depths of the Clarion-Clipperton Fracture Zone, North Equatorial Pacific Ocean. *Zootaxa* 4629 (2): 151–87. https://doi.org/10.11646/zootaxa.4629.2.1

Böggemann M. 2009. Polychaetes (Annelida) of the abyssal SE Atlantic. *Organisms Diversity & Evolution* 9 (4–5): 251–428.

Böggemann M. & Purschke G. 2005. Abyssal benthic Syllidae (Annelida: Polychaeta) from the Angola Basin. *Organisms Diversity & Evolution* 5 (Supp. 1): 221–226. https://doi.org/10.1016/j.ode.2004.11.006

Bonifácio P. & Menot L. 2018. New genera and species from the Equatorial Pacific provide phylogenetic insights into deep-sea Polynoidae (Annelida). *Zoological Journal of the Linnean Society* 185 (3): 555–635. https://doi.org/10.1093/zoolinnean/zly063

Bonifácio P., Martínez Arbizu P. & Menot L. 2020. Alpha and beta diversity patterns of polychaete assemblages across the nodule province of the eastern Clarion-Clipperton Fracture Zone (equatorial Pacific). *Biogeosciences* 17 (4): 865–886. https://doi.org/10.5194/bg-17-865-2020

Bonifácio P., Kaiser S., Washburn T.W., Smith C.R., Vink A. & Martínez Arbizu P. 2024. Biodiversity of the Clarion-Clipperton Fracture Zone: a worm perspective. *Marine Biodiversity* 54 (1): 5. https://doi.org/10.1007/s12526-023-01396-3

Carr C.M., Hardy S.M., Brown T.M., Macdonald T.A. & Hebert P.D. 2011. A tri-oceanic perspective: DNA barcoding reveals geographic structure and cryptic diversity in Canadian polychaetes. *PLoS ONE* 6 (7): e22232. https://doi.org/10.1371/journal.pone.0022232

Cohen B.L., Gawthrop A. & Cavalier-Smith T. 1998. Molecular phylogeny of brachiopods and phoronids based on nuclear-encoded small subunit ribosomal RNA gene sequences. *Philosophical Transactions of the Royal Society of London. Series B: Biological Sciences* 353 (1378): 2039–2061. https://doi.org/10.1098/rstb.1998.0351

Dales R.P. 1962. The polychaete stomodeum and the inter-relationships of the families of Polychaeta. *Proceedings of the Zoological Society of London* 139 (3): 389–428. https://doi.org/10.1111/j.1469-7998.1962.tb01837.x

Darriba Di., Posada D., Kozlov A.M., Stamatakis A., Morel B. & Flouri T. 2020. ModelTest-NG: A new and scalable tool for the selection of DNA and protein evolutionary models. *Molecular Biology and Evolution* 37 (1): 291–294. https://doi.org/10.1093/MOLBEV/MSZ189

Day J.H. 1963. The annelid fauna of South Africa. Part 8: new species and records from grab samples and dredgings. *Bulletin of the British Museum (Natural History), Series Zoology* 10 (7): 381–445. https://doi.org/10.5962/bhl.part.20530

Dean H.K. 2008. The use of annelid (Annelida) as indicator species of marine pollution: a review. *Revista de Biología Tropical* 56(4): 11–38

Drennan R., Wiklund H., Rabone M., Georgieva M.N., Dahlgren T.G. & Glover A.G. 2021. *Neanthes goodayi* sp. nov. (Annelida, Nereididae), a remarkable new annelid species living inside deep-sea polymetallic nodules. *European Journal of Taxonomy* 760: 160–185. https://doi.org/10.5852/ejt.2021.760.1447

Drennan R., Neal L., Wiklund H., Stewart E.C., Rabone M., Boolukos C., Clatworthy I., Jungmanova Z., Dahlgren T.G. & Glover A.G. 2025. On *Anguillosyllis* cf. *hessleri* Maciolek, 2020 – A species complex from the Clarion-Clipperton zone, abyssal central Pacific. *Deep Sea Research Part I: Oceanographic Research Papers* 220: 104453. https://doi.org/10.1016/j.dsr.2025.104453

Edgar R.C. 2004. MUSCLE: multiple sequence alignment with high accuracy and high throughput. *Nucleic Acids Research* 32 (5): 1792–1797. https://doi.org/10.1093/nar/gkh340

Folmer O., Black M., Hoeh W., Lutz R. & Vrijenhoek R. 1994. DNA primers for amplification of mitochondrial cytochrome c oxidase subunit I from diverse metazoan invertebrates. *Molecular Marine Biology Biotechnology* 3 (5): 294–299.

Glover A.G., Smith C.R., Paterson G.L., Wilson G.D., Hawkins L. & Sheader M. 2002. Annelid species diversity in the central Pacific abyss: local and regional patterns, and relationships with productivity. *Marine Ecology Progress Series* 240: 157–170. https://doi.org/10.3354/meps240157

Glover A.G., Dahlgren T.G., Wiklund H., Mohrbeck I. & Smith C.R. 2016. An end-to-end DNA taxonomy methodology for benthic biodiversity survey in the Clarion-Clipperton Zone, Central Pacific abyss. *Journal of Marine Science and Engineering* 4 (1): e2. https://doi.org/10.3390/jmse4010002

Glover A.G., Wiklund H., Chen C. & Dahlgren T.G. 2018. Point of view: managing a sustainable deep-sea "blue economy" requires knowledge of what actually lives there. *eLife* 7: e41319. https://doi.org/10.7554/eLife.41319

Gollner S., Kaiser S., Menzel L., Jones D.O.B., Brown A., Mestre N.C., Van Oevelen D., Menot L., Colaço A., Canals M., Cuvelier D., Durden J.M., Gebruk A., Egho G.A., Haeckel M., Marcon Y., Mevenkamp L., Morato T., Pham C.K., Purser A. & Martínez Arbizu P. 2017. Resilience of benthic deep-sea fauna to mining activities. *Marine Environmental Research* 129: 76–101. https://doi.org/10.1016/j.marenvres.2017.04.010

Grube A.E. 1850. Die Familien der Anneliden. *Archiv für Naturgeschichte* 16 (1): 249–364. Available from https://biodiversitylibrary.org/page/6958350 [accessed 9 Sep. 2025].

Guggolz T., Meißner K., Schwentner M., Dahlgren T.G., Wiklund H., Bonifácio P. & Brandt A. 2020. High diversity and pan-oceanic distribution of deep-sea polychaetes: *Prionospio* and *Aurospio* (Annelida: Spionidae) in the Atlantic and Pacific Ocean. *Organisms Diversity & Evolution* 20: 171–187. https://doi.org/10.1007/s13127-020-00430-7

Gunton L.M., Kupriyanova E.K., Alvestad T., Avery L., Blake J.A., Biriukova O., Böggemann M., Borisova P., Budaeva N., Burghardt I., Capa M., Georgieva M.N., Glasby C.J., Hsueh P.-W., Hutchings P., Jimi N., Kongsrud J.A., Langeneck J., Meißner K., ... & Zhang J. 2021. Annelids of the eastern Australian abyss collected by the 2017 RV 'Investigator'voyage. *ZooKeys* 1020: 1–198. https://doi.org/10.3897/zookeys.1020.57921

Hartman O. 1965. Deep-water *benthic* polychaetous annelids off New England to Bermuda and other North Atlantic areas. *Allan Hancock Foundation Publications*, *Occasional Paper* 28: 1–378. https://doi.org/10.25549/hancock-c82-20299

Hartman O. 1967. Polychaetous annelids collected by the USNS Eltanin and Staten Island cruises, chiefly from Antarctic seas. *Allan Hancock Monographs in Marine Biology* 2: 1–387.

Hoang D.T., Chernomor O., von Haeseler A., Minh B.Q. & Vinh L.S. 2018. UFBoot2: improving the ultrafast bootstrap approximation. *Molecular Biology and Evolution* 35 (2): 518–522. https://doi.org/10.1093/molbev/msx281

Janssen A., Kaiser S., Meissner K., Brenke N., Menot L. & Martínez Arbizu P. 2015. A reverse taxonomic approach to assess macrofaunal distribution patterns in abyssal Pacific polymetallic nodule fields. *PLoS ONE* 10 (2): e0117790. https://doi.org/10.1371/journal.pone.0117790

Johnson M., Zaretskaya I., Raytselis Y., Merezhuk Y., McGinnis S. & Madden T. L. 2008. NCBI BLAST: a better web interface. *Nucleic Acids Research* 36 (suppl_2): W5–W9. https://doi.org/10.1093/NAR/GKN201

Jones D.O., Simon-Lledó E., Amon D.J., Bett B.J., Caulle C., Clément L., Connelly D.P., Dahlgren T.G., Durden J.M., Drazen J.C., Felden J., Gates A.R., Georgieva M.N., Glover A.G., Gooday A.J., Hollingsworth A.L., Horton T., James R.H., Jeffreys R.M., ... & Huvenne V.A.I. 2021. Environment, ecology, and potential effectiveness of an area protected from deep-sea mining (Clarion Clipperton Zone, abyssal Pacific). *Progress in Oceanography* 197: 102653. https://doi.org/10.1016/j.pocean.2021.102653

Kalyaanamoorthy S., Minh B.Q., Wong T.K.F., von Haeseler A. & Jermiin L.S. 2017. ModelFinder: fast model selection for accurate phylogenetic estimates. *Nature Methods* 14: 587–589. https://doi.org/10.1038/nmeth.4285

Katoh K. 2002. MAFFT: a novel method for rapid multiple sequence alignment based on fast Fourier transform. *Nucleic Acids Research* 30 (14): 3059–3066. https://doi.org/10.1093/nar/gkf436

Kearse M., Moir R., Wilson A., Stones-Havas S., Cheung M., Sturrock S., Buxton S., Cooper A., Markowitz S., Duran C., Thierer T., Ashton B., Meintjes P. & Drummond A. 2012. Geneious Basic: an integrated and extendable desktop software platform for the organization and analysis of sequence data. *Bioinformatics* 28 (12): 1647–1649. https://doi.org/10.1093/bioinformatics/bts199

Kimura M. 1980. A simple method for estimating evolutionary rates of base substitutions through comparative studies of nucleotide sequences. *Journal of Molecular Evolution* 16: 111–120. https://doi.org/10.1007/BF01731581

Lamarck J.B. de 1802. [privately published, reprinted 1906]). Discours d'Ouverture, Prononcé le 27 floréal An 10, au Muséum d'Histoire naturelle. Recherches sur l'organisation des corps vivans. [reprint 1906] *Bulletin scientifique de la France et de la Belgique (5th series)* 40: 483–517 [Les Annelides p. 494]. Available from https://gallica.bnf.fr/ark:/12148/bpt6k4226016j, https://www.biodiversitylibrary.org/page/10730977, http://redi.imss.fi.it/lamarck/ouvrages/docpdf/Recherches_organisation.pdf [accessed 9 Sep. 2025].

Langeneck J., Musco L., Busoni G., Conese I., Aliani S. & Castelli A. 2018. Syllidae (Annelida: Phyllodocida) from the deep Mediterranean Sea, with the description of three new species. *Zootaxa* 4369 (2): 197–220. https://doi.org/10.11646/ZOOTAXA.4369.2.3

Langerhans P. 1879. Die Wurmfauna von Madeira [part I]. *Zeitschrift für wissenschaftliche Zoologie* 32 (4): 513–592. Available from https://www.biodiversitylibrary.org/page/45240737 [accessed 9 Sep. 2025].

Lodge M., Johnson D., Le Gurun G., Wengler M., Weaver P. & Gunn V. 2014. Seabed mining: International Seabed Authority environmental management plan for the Clarion-Clipperton Zone. A partnership approach. *Marine Policy* 49: 66–72. https://doi.org/10.1016/j.marpol.2014.04.006

Maciolek N.J. 2020. *Anguillosyllis* (Annelida: Syllidae) from multiple deep-water locations in the northern and southern hemispheres. *Zootaxa* 4793 (1): 1–73. https://doi.org/10.11646/ZOOTAXA.4793.1.1

Malaquin A. 1893. Recherches sur les Syllidiens. Morphologie, anatomie, reproduction, développement. *Mémoires de la Société des Sciences, de l'Agriculture et des Arts de Lille 4e Série* 18: 1–477. https://doi.org/10.5962/bhl.title.99327

Medlin L., Elwood H.J., Stickel S. & Sogin M.L. 1988. The characterization of enzymatically amplified eukaryotic 16S-like rRNA-coding regions. *Gene* 71 (2): 491–499. https://doi.org/10.1016/0378-1119(88)90066-2

Minh B.Q., Nguyen M.A.T. & von Haeseler A. 2013. Ultrafast approximation for phylogenetic bootstrap. *Molecular Biology and Evolution* 30 (5): 1188–1195. https://doi.org/10.1093/molbev/mst024

Neal L., Paterson G.L., Blockley D., Scott B., Sherlock E., Huque C. & Glover A.G. 2020. Biodiversity data and new species descriptions of polychaetes from offshore waters of the Falkland Islands, an area undergoing hydrocarbon exploration. *ZooKeys* 938: 1–86. https://doi.org/10.3897/zookeys.938.49349

Neal L., Wiklund H., Rabone M., Dahlgren T.G. & Glover A.G. 2022a. Abyssal fauna of polymetallic nodule exploration areas, eastern Clarion-Clipperton Zone, central Pacific Ocean: Annelida: Spionidae and Poecilochaetidae. *Marine Biodiversity* 52 (5): 51. https://doi.org/10.1007/s12526-022-01277-1

Neal L., Wiklund H., Gunton L.M., Rabone M., Bribiesca-Contreras G., Dahlgren T.G. & Glover A.G. 2022b. Abyssal fauna of polymetallic nodule exploration areas, eastern Clarion-Clipperton Zone, central

Pacific Ocean: Amphinomidae and Euphrosinidae (Annelida, Amphinomida). *ZooKeys* 1137: 33–74. https://doi.org/10.3897/zookeys.1137.86150

Neal L., Abrahams E., Wiklund H., Rabone M., Bribiesca-Contreras G., Stewart E.C., Dahlgren T.G. & Glover A.G. 2023. Taxonomy, phylogeny, and biodiversity of Lumbrineridae (Annelida, Polychaeta) from the Central Pacific Clarion-Clipperton Zone. *ZooKeys* 1172: 61–100. https://doi.org/ 10.3897/zookeys.1172.100483

Nilsson C.L., Wiklund H., Glover A.G., Bribiesca-Contreras G. & Dahlgren T.G. 2024. A new species of *Erinaceusyllis* (Annelida: Syllidae) discovered at a wood-fall in the eastern Clarion-Clipperton zone, central Pacific Ocean. *Deep Sea Research Part I: Oceanographic Research Papers* 214: 104415. https://doi.org/10.1016/j.dsr.2024.104415

Nygren A. & Sundberg P. 2003. Phylogeny and evolution of reproductive modes in Autolytinae (Syllidae, Annelida). *Molecular Phylogenetics and Evolution* 29 (2): 235–249. https://doi.org/10.1016/S1055-7903(03)00095-2

Palumbi S.R. 1996. Nucleic acids II: The polymerase chain reaction. *In*: Hillis D.M., Moritz C. & Mable B.K. (eds). *Molecular Systematics* 2 (1): 205–247. Sinauer, Sunderland, MA.

Paterson G.L., Neal L., Altamira I., Soto E.H., Smith C.R., Menot L., Billett D.S., Cunha M.R., Marchais-Laguionie C. & Glover A.G. 2016. New *Prionospio* and *Aurospio* species from the deep sea (Annelida: Polychaeta). *Zootaxa* 4092 (1):1–32. https://doi.org/10.11646/zootaxa.4092.1.1

Rabone M., Horton T., Jones D.O., Simon-Lledó E. & Glover A.G. 2023a. A review of the International Seabed Authority database DeepData from a biological perspective: challenges and opportunities in the UN Ocean Decade. *Database* 2023: baad013. https://doi.org/10.1093/database/baad013

Rabone M., Wiethase J.H., Simon-Lledó E., Emery A.M., Jones D.O., Dahlgren T.G., Bribiesca-Contreras L., Wiklund H., Horton T. & Glover A.G. 2023b. How many metazoan species live in the world's largest mineral exploration region? *Current Biology* 33: 1–14. https://doi.org/10.1016/j.cub.2023.04.052

Rambaut A. 2018. FigTree – Tree Figure Drawing Tool v. 1.4.4. Institute of Evolutionary Biology, University of Edinburgh, Edinburgh. Available from https://tree.bio.ed.ac.uk/software/figtree/ [accessed 9 Sep. 2025].

Ronquist F., Teslenko M., Van Der Mark P., Ayres D.L., Darling A., Höhna S., Larget B., Liu L., Suchard M.A. & Huelsenbeck J.P. 2012. MrBayes 3.2: efficient Bayesian phylogenetic inference and model choice across a large model space. *Systematic Biology* 61 (3): 539–542. https://doi.org/10.1093/sysbio/sys029

Sjölin E., Erséus C. & Källersjö M. 2005. Phylogeny of Tubificidae (Annelida, Clitellata) based on mitochondrial and nuclear sequence data. *Molecular Phylogenetics and Evolution* 35 (2): 431–441. https://doi.org/10.1016/j.ympev.2004.12.018

Smith C.R., De Leo F.C., Bernardino A.F., Sweetman A.K. & Martínez Arbizu P. 2008. Abyssal food limitation, ecosystem structure and climate change. *Trends in Ecology and Evolution* 23 (9): 518–28. https://doi.org/10.1016/j.tree.2008.05.002

Smith C.R., Paterson G., Lambshead J., Glover A., Rogers A., Gooday A., Kitazato H., Sibuet M., Galeron J. & Menot L. 2011. *Biodiversity, Species Ranges, and Gene Flow in the Abyssal Pacific Nodule Province: Predicting and Managing the Impacts of Deep Seabed Mining*. ISA Technical Study No. 3. International Seabed Authority, Kingston, Jamaica.

Smith C.R., Clark M.R., Goetze E., Glover A.G. & Howell K.L. 2021. Biodiversity, connectivity and ecosystem function across the Clarion-Clipperton Zone: A regional synthesis for an area targeted for nodule mining. *Frontiers in Marine Science* 8: e797516. https://doi.org/10.3389/fmars.2021.797516

Stewart E.C.D., Bribiesca-Contreras G., Taboada S., Wiklund H., Ravara A., Pape, E., De Smet B., Neal L., Cunha M.R., Jones D.O.B., Smith C.R., Glover A.C. & Dahlgren T.G. 2023. Biodiversity, biogeography, and connectivity of polychaetes in the world's largest marine minerals exploration frontier. *Diversity and Distributions* 29 (6): 727–747. https://doi.org/10.1111/ddi.13690

Tamura K., Stecher G. & Kumar S. 2021. MEGA11: Molecular Evolutionary Genetics Analysis Version 11. *Molecular Biology and Evolution* 38 (7): 3022–3027. https://doi.org/10.1093/MOLBEV/MSAB120

Trifinopoulos J., Nguyen L.T., von Haeseler A. & Minh B.Q. 2016. W-IQ-TREE: A fast online phylogenetic tool for maximum likelihood analysis. *Nucleic Acids Research* 44 (W1): W232–W235. https://doi.org/10.1093/nar/gkw256

Washburn T.W., Jones D.O., Wei C.L. & Smith C.R. 2021. Environmental heterogeneity throughout the Clarion-Clipperton Zone and the potential representativity of the APEI network. *Frontiers in Marine Science* 8: 661685. https://doi.org/10.3389/fmars.2021.661685

Wiklund H., Neal L., Glover A.G., Drennan R., Rabone M. & Dahlgren T.G. 2019. Abyssal fauna of polymetallic nodule exploration areas, eastern Clarion-Clipperton Zone, central Pacific Ocean: Annelida: Capitellidae, Opheliidae, Scalibregmatidae, and Travisiidae. *ZooKeys* 883: 1–82. https://doi.org/10.3897/zookeys.883.36193

Wiklund H., Rabone M., Glover A., Bribiesca-Contreras G., Drennan R., Stewart E., Boolukos C., King L., Sherlock E., Smith C., Dahlgren T. & Neal L. 2023. Checklist of newly-vouchered annelid taxa from the Clarion-Clipperton Zone, central Pacific Ocean, based on morphology and genetic delimitation. *Biodiversity Data Journal* 11: e86921. https://doi.org/10.3897/BDJ.11.e86921

Wilson G.D. 2017. Macrofauna abundance, species diversity and turnover at three sites in the Clipperton-Clarion Fracture Zone. *Marine Biodiversity* 47 (2): 323–347. https://doi.org/10.1007/s12526-016-0609-8

Printed versions of all papers are deposited in the libraries of three of the institutes that are members of the EJT consortium: Muséum national d'Histoire naturelle, Paris, France; Royal Museum for Central Africa, Tervuren, Belgium; Royal Belgian Institute of Natural Sciences, Brussels, Belgium. The other members of the consortium are: Meise Botanic Garden, Meise, Belgium; Natural History Museum of Denmark, Copenhagen, Denmark; Naturalis Biodiversity Center, Leiden, the Netherlands; Museo Nacional de Ciencias Naturales-CSIC, Madrid, Spain; Leibniz Institute for the Analysis of Biodiversity Change, Bonn – Hamburg, Germany; National Museum of the Czech Republic, Prague, Czech Republic; The Steinhardt Museum of Natural History, Tel Aviv, Israël.

Supplementary files

Supp. file 1. Table S1. List of sequences from GenBank used in phylogenetic analyses. https://doi.org/10.5852/ejt.2025.1026.3105.13849

Supp. file 2. Table S2. GenBank numbers for phylogenetic analysis data downloaded from GenBank. https://doi.org/10.5852/ejt.2025.1026.3105.13851

Supp. file 3. Fig. S1. Phylogenetic analysis of *Anguillosyllis* Day, 1963 using the 16S RNA barcode marker. New species described in this study are highlighted in bold and colour. The tree also includes representatives of the *Anguillosyllis* cf. *hessleri* species complex described in Drennan *et al.* (2025), in addition to nine *Anguillosyllis*, ten syllid and three non-syllid nereidiform outgroup sequences from GenBank. Support values are given at nodes as maximum likelihood (ML) bootstrap values.
https://doi.org/10.5852/ejt.2025.1026.3105.13853

Supp. file 4. Fig. S2. Phylogenetic analysis of *Anguillosyllis* Day, 1963 using the Cytochrome Oxidase Subunit I (COI) barcode marker. New species described in this study are highlighted in bold and colour. The tree also includes representatives of the *Anguillosyllis* cf. *hessleri* species complex described in Drennan *et al.* (2025), in addition to nine *Anguillosyllis*, ten syllid and three non-syllid nereidiform outgroup sequences from GenBank. Support values are given at nodes as maximum likelihood (ML) bootstrap values. https://doi.org/10.5852/ejt.2025.1026.3105.13855